Quaternary Science Reviews 329 (2024) 108561

Contents lists available at ScienceDirect

Quaternary Science Reviews

journal homepage: www.elsevier.com/locate/quascirev

Not seen before. Unveiling depositional context and *Mammuthus meridionalis* exploitation at Fuente Nueva 3 (Orce, southern Iberia) through taphonomy and microstratigraphy

José Yravedra [a,b,c,d,e,**], Lloyd A. Courtenay [f,***], Mario Gutiérrez-Rodríguez [g], Juan Francisco Reinoso-Gordo [h], Juha Saarinen [i], Natalia Égüez [j], Carmen Luzón [k], Juan José Rodríguez-Alba [a], José A. Solano [k], Stefania Titton [l,m], Eva Montilla-Jiménez [k,e], José Cámara-Donoso [i,k], Darío Herranz-Rodrigo [k], Verónica Estaca [a], Alexia Serrano-Ramos [k], Gabriela Amorós [n], Beatriz Azanza [o,p], Hervé Bocherens [q], Daniel DeMiguel [o,p,r,s], Ana Fagoaga [l,t,u], Antonio García-Alix [v], Juan José González-Quiñones [h,k], Francisco Jiménez-Espejo [w], Anu Kaakinen [i], Manuel Munuera [x], Juan Ochando [n], Pedro Piñero [l], Christian Sánchez-Bandera [l,m], Suvi Viranta [y], Mikael Fortelius [i,z,aa], Jordi Agustí [l,m,ab], Hugues-Alexandre Blain [l,m], José Carrión [n], Deborah Barsky [l,m], Oriol Oms [ac], Carolina Mallol [j], Juan Manuel Jiménez-Arenas [k,ad,ae,e,*]

[a] *Departamento de Prehistoria, Historia Antigua y Arqueología. Universidad Complutense, Madrid, Spain*
[b] *Centro de Asistencia e Investigación 'Ciencias de la Tierra y Arqueometría', Unidad de Arqueometría y Análisis Arqueológico, Universidad Complutense, Madrid, Spain*
[c] *Grupo de Investigación Ecosistemas Cuaternarios. Universidad Complutense, Madrid, Spain*
[d] *Grupo de Investigación Arqueología Prehistórica. Universidad Complutense, Madrid, Spain*
[e] *Museo Primeros Pobladores de Europa 'Josep Gibert', Orce, Granada, Spain*
[f] *CNRS, PACEA UMR 5199, Université de Bordeaux, France*
[g] *Instituto Universitario de Investigación en Arqueología Ibérica. Universidad de Jaén, Spain*
[h] *Departamento de Expresión Gráfica Arquitectónica y en la Ingeniería, Universidad de Granada, Granada, Spain*
[i] *Department of Geosciences and Geology, University of Helsinki, Helsinki, Finland*
[j] *Archaeological Micromorphology and Biomarkers Research Lab (AMBILAB), Instituto Universitario de Bio-Orgánica Antonio González, Universidad de La Laguna, Santa Cruz de Tenerife, Spain*
[k] *Departamento de Prehistoria y Arqueología, Universidad de Granada, Granada, Spain*
[l] *Institut Català de Paleoecologia Humana i Evolució Social (IPHES-CERCA), Tarragona, Spain*
[m] *Departament d'Història i Història de l'Art, Universitat Rovira i Virgili, Tarragona, Spain*
[n] *Departamento de Botánica, Universidad de Murcia, Murcia, Spain*
[o] *Departamento de Ciencias de la Tierra, Universidad de Zaragoza, Zaragoza, Spain*
[p] *Instituto Universitario de Investigación en Ciencias Ambientales de Aragón (IUCA), Universidad de Zaragoza, Zaragoza, Spain*
[q] *Universität Tübingen and Senckenberg Centre for Human Evolution and Palaeoenvironment, Tübingen, Germany*
[r] *Fundación Agencia Aragonesa para la Investigación y el Desarrollo (ARAID), Zaragoza, Spain*
[s] *Institut Català de Paleontologia Miquel Crusafont, Universitat Autònoma de Barcelona, Barcelona, Spain*
[t] *Grupo de Investigación en Paleontología de Vertebrados Cenozoicos, Àrea de Palaeontologia, Universitat de València, Valencia, Spain*
[u] *Museu Valencià d'Història Natural, Valencia, Spain*
[v] *Departamento de Estratigrafía y Paleontología, Universidad de Granada, Granada, Spain*
[w] *Instituto Andaluz de Ciencias de la Tierra (IACT), Consejo Superior de Investigaciones Científicas-Universidad de Granada (CSIC-UGR), Granada, Spain*
[x] *Departamento de Ingeniería Agronómica, Universidad Politécnica de Cartagena, Cartagena, Murcia, Spain*
[y] *Department of Anatomy, University of Helsinki, Helsinki, Finland*
[z] *Finnish Museum of Natural History, Helsinki, Finland*
[aa] *Visiting Scholars Program, Departamento de Prehistoria y Arqueología, Universidad de Granada, Granada, Spain*
[ab] *Institució Catalana de Recerca i Estudis Avançats (ICREA), Barcelona, Spain*
[ac] *Departament de Geologia, Universitat Autònoma de Barcelona, Cerdanyola del Vallés, Barcelona, Spain*
[ad] *Unidad de Excelencia 'Archaeometrical Studies. Inside the Artefacts & Ecofacts', Universidad de Granada, Granada, Spain*

* Corresponding author. Departamento de Prehistoria y Arqueología, Universidad de Granada, Granada, Spain.
** Corresponding author. Departamento de Prehistoria, Historia Antigua y Arqueología, Universidad Complutense, Madrid, Spain.
*** Corresponding author.
E-mail addresses: jyravedr@ucm.es (J. Yravedra), lloyd.courtenay@u-bordeaux.fr (L.A. Courtenay), jumajia@ugr.es (J.M. Jiménez-Arenas).

https://doi.org/10.1016/j.quascirev.2024.108561
Received 15 October 2023; Received in revised form 6 January 2024; Accepted 20 February 2024
Available online 4 March 2024

[ae] The Gibraltar Museum, Gibraltar, United Kingdom

ARTICLE INFO

Handling Editor: Danielle Schreve

Keywords:
Early *Homo*
Machairodontine felids
Taphonomy
Micromorphology
Geometric morphometrics

ABSTRACT

Meat consumption by early hominins is a hotly debated issue. A key question concerns their access to large mammal carcasses, including megafauna. Currently, the evidence of anthropic cut marks on proboscidean bones older than -or close to- 1.0 Ma are restricted to the archaeological sites of Dmanisi (Georgia), Olduvai (Tanzania), Gona (Ethiopia), Olorgesailie (Kenya) and La Boella (Spain). During an inspection of the almost complete carcass of *Mammuthus meridionalis* (FN3-5-MPS) from the Oldowan site of Fuente Nueva 3 (Orce, Spain, *c.* 1.2 Ma), a few traces compatible with human-made cut marks and carnivore tooth marks were found. From this finding and previous interpretations the following questions arise: When and under what conditions was FN3-5-MPS deposited? What is the nature of the marks found on the surface of the bones of this mammoth? To answer, we have conducted a high-resolution analysis of these remains, combining both taphonomic and microstratigraphic data. Our results, using microstratigraphic and micromorphological analyses of sediments based on thin-sections, show that this individual was deposited in a marshy environment. Subsequently, the carcass was exploited by hominins and large felids that left their marks on the surface of some of its bones. For this purpose, the identification and characterisation of both cut marks and tooth marks were performed using high-resolution 3D modelling, geometric morphometrics, and artificially intelligent algorithms. Based on the anatomical position of both the cut and tooth marks, we propose that both the hominins and the saber-toothed cats had early access to the animal. Finally, this paper shows how an interdisciplinary approach can shed detailed light on the particular story regarding the death and processing of the carcass of a female mammoth, deposited at Fuente Nueva 3.

1. Introduction

The acquisition and consumption of animal resources linked to large mammals has occupied an important place in human evolution (e.g. Agam and Barkai, 2018; Haynes, 1991, 2017, 2022; Linares-Matás and Yravedra, 2021). Regarding megafauna, classic interpretations by Aguilera-Gamboa (1913) were later illustrated by the iconic drawings of Burian (Spinar, 1996), and popularized by Butzer, Freeman, and Howell, who interpreted that hominins drove elephants to swampy areas where they could hunt them (Freeman and Butzer, 1966; Howell, 1966; Freeman and Howell, 1981; Howell and Freeman, 1982, 1983). While some evidence has also been described for sites older than a million years (Haynes, 2022), such behaviour is more common in the Middle and Upper Paleolithic (Yravedra et al., 2019; Haynes, 2022), and in particular during the Late Pleistocene (Surovell et al., 2005; Agam and Barkai, 2018; Wojtal et al., 2019; Gaudzinski-Windheuser et al., 2023).

Identifying when a given taxon, including humans, have consumed an animal carcass requires very specific kind of evidence. It is not uncommon for casual associations to occur between lithic industries and proboscidean bones in archaeological sites. Critical analyses by, for example, Isaac and Crader (1981, 1983) and Domínguez-Rodrigo et al. (2007), showed fortuitous associations of proboscidean remains with lithic industries in FLK N6 (Bed I) and FLK N (Bed II, Olduvai Gorge, Tanzania). Likewise, (Haynes et al. 2020a, b) also dismissed the anthropogenic character of sites such as Lamb Spring (Colorado, USA), Lovewell (Kansas, USA), and La Sena (Nebraska, USA). One of the most reliable means of confirming associations between lithic and megafaunal remains thus mostly lies on taphonomic evidence, such as the direct identification of cut and percussion marks on these elements (e.g. Yravedra et al., 2019; Haynes, 2022) or, in more recent contexts, impact marks produced by projectile points (Surovell et al., 2005; Waters et al., 2011).

Some of the earliest evidence of cut marks on the surface of proboscidean bones predating 1 Ma are documented from Olduvai Gorge (Tanzania). Early examples include cut marks identified on the dorsal surface of a proboscidean talus bone from HWK EE (Bed II, *c.* 1.7 Ma) (de la Torre et al., 2018; Pante and de la Torre, 2018), cut marks on proboscidean remains from BK (Upper Bed II) (Monahan, 1996), as well as two, likely anthropogenic, proboscidean bone flakes from BK4b, associated with cut marked megafaunal remains (Upper Bed II, *c.* 1.34 Ma) (Domínguez-Rodrigo et al., 2014). Other Olduvai sites, such as JK (Bed III, *c.* 1.15–0.80 Ma) have provided megafaunal (likely proboscidean) remains with evidence of percussion marks (Yravedra et al., 2020). Elsewhere, Early Pleistocene examples dating *c.* 1.6–1.5 Ma include Dan Aoule North 5 (Gona, Ethiopia), with cut marks on a proximal phalanx of *Elephas* (Semaw et al., 2020), while the transition to Middle Pleistocene presents examples of cut marked *Palaeoloxodon recki* ribs from Olorgesailie (Site 19 of Member 1, *c.* 1 Ma, Kenya) (Potts et al., 1999).

An additional intriguing association between lithic artifacts and proboscidean remains has been documented in Barogali (Republic of Djibouti, *c.* 1.6–1.3 Ma) (Chavaillon et al., 1986; Berthelet and Chavaillon, 2001; Berthelet, 2002). This example is composed by a lithic assemblage of 569 artifacts, many of which are configured for fracturing activities, alongside an almost complete skeleton of *P. recki*. Some parts of the proboscidean appear in anatomical connection, others in semi-connection, and many scattered over a not too large area (Berthelet and Chavaillon, 2001). Specifically, the appearance of the cranial calotte well separated from the rest of the skull led Berthelet and Chavaillon (2001) to propose that it was intentionally fractured to access the brain. Nevertheless, no direct evidence of fracturing or cutting has been directly documented on these remains. Likewise, a similar example can be observed with the Middle Pleistocene site of Ndung'a (Kenya, *c.* 0.7 Ma), where spatial association between proboscidean and abundant lithic remains has been documented. Nevertheless, in this latter case study, no taphonomic evidence is preserved directly linking the two (Delagnes et al., 2006).

Outside of Africa, the oldest evidence of hominin processing of a proboscidean carcass is found at Dmanisi (Georgia, 1.8 Ma), where a *Mammuthus meridionalis* rib presents cut marks on the proximal epiphysis (Tappen et al., 2022). This is followed by the example of Pit 1 in Barranc de la Boella (Tarragona, Spain), an Acheulean site dated at 990-780 ka, presenting two *M. meridionalis* ribs with preserved anthropogenic modifications in the form of cut marks (Mosquera et al., 2015). These finds are accompanied by the documentation of furrowing observed on the proximal epiphysis of a mammoth tibia, as well as a metapodial turned into a cylinder by carnivore activity (Pineda et al., 2017).

Alongside these examples, Fuente Nueva 3 (FN3, Orce, Spain) is another key site attracting the attention of specialists, presenting the spatial association between coprolites, knapped lithic implements, and proboscidean remains. The partial skeleton FN3-5-MPS (Fig. 1) stands out among the abundant *M. meridionalis* individuals recovered and

Fig. 1. Cast of the individual FN3-5-MPS on display in the Museo Primeros Pobladores de Europa Josep Gibert (Orce, Granada, Spain). Scale = 100 cm (each section of the archaeological marker represents 10 cm).

extracted so far from this site. These remains were unearthed in Level 5, during 3 field seasons between 2001 and 2003, and published as belonging to a single individual deposited in a thick layer of fine sands formed during a short sedimentary event at the shore of the paleo lake Baza (Espigares et al., 2013, 2023; Palmqvist et al., 2023). This discovery is comprised of most of the axial skeleton (18 vertebrae, 14 ribs, the right scapula and the almost complete pelvis), as well as the mandible, while the cranium and appendicular limb bones are absent. This find since been interpreted as evidence of selective transport of the appendicular skeleton by humans (Espigares et al., 2013). Likewise, the presence of coprolites ($n = 34$), some of which are clearly in the greenish sandy facies of FN3-5 (see Fig. 6A in Espigares et al., 2013), and knapped lithic implements ($n = 17$ according to Espigares et al., 2013; $n = 27$ in Palmqvist et al., 2023), found in proximity with FN3-5-MPS, have been interpreted as evidence of competition between hyenas and humans for access to the proboscidean carcass.

To date, no published taphonomic data is available to directly associate the carcass with either carnivoran or hominin biotic agents. Specifically, Espigares et al. (2013) claim that "*tooth marks are absent from the* M. meridionalis *carcass from Fuente Nueva-3*" (Espigares et al., 2013:117). Furthermore, Palmqvist et al. (2023) state that it is not possible to find cut or tooth marks on the cortical surface of FN3-5-MPS based on the following arguments;

1. The periosteum of proboscidean long bones is too thick for marks to be left on bone.
2. Saber-toothed cats do not leave tooth marks because their delicate dentition may break and compromise their survival.
3. The absence of cut and tooth marks is due to the bad preservation conditions during the 3 years period (2001–2003) during which the FN3-5-MPS individual was exhumed. This considers the oscillation between summer-winter periods in Orce to be particularly problematic for partially exposed remains.

Nevertheless, field observations of the stratigraphy of FN3, and in particular FN3-5, indicate this level to be considerably complex. Recent studies have been able to identify three different sublevels within the FN3-5 stratigraphic unit (Yravedra et al., 2021), while the fact that the lithics and the bones appear at the same stratigraphic level, sublevel or even microfacies, do not mean that they were deposited at the same time. For these reasons, we must consider the contextual and temporal resolution limits of Pleistocene archaeology itself; the synchronous association of complex human and biotic activities occurring in specific events at Pleistocene sites is very challenging. This is true not only considering the case of palimpsests and complex sedimentary processes, but also site formation processes before, during, and after the deposition of fossil remains.

In light of this, and in the absence of direct evidence (cut marks, tooth marks, etc.), we cannot discard that the association of proboscidean bones, lithic tools, and coprolites, could be product of mere circumstance (e.g. Haynes, 1991; Chazan and Horwitz, 2006; Yravedra et al., 2014, 2019; Haynes et al., 2020a, b). To avoid falling into the so-called 'Pompeii Premise' — the mistaken assumption that archaeological assemblages are a faithful reflection of a specific moment in the past (Ascher, 1961; Binford, 1981; Schiffer, 1985) — it is necessary to explore the genesis of the archaeological record at a high resolution, combining both microstratigraphic and taphonomic data.

The purpose of this research is to therefore present a re-evaluation of the proboscidean remains corresponding to FN3-5-MPS housed at the Museo Primeros Pobladores de Europa 'Josep Gibert' (Orce, Granada, Spain). Considering the most recent publications about FN3, alongside the aforementioned debate on proboscidean remains, several questions arise: How complex is the so-called 'FN3-Level 5'? In which microfacies of the stratigraphic unit was FN3-5-MPS deposited? Are all the coprolites surrounding the skeleton in the same stratigraphic facies? Are the traces found on FN3-5-MPS possible cut marks or trampling marks? Can the carnivoran damage be attributed to any particular carnivoran? For this purpose, here we conduct a high-resolution analysis of the taphonomic remains which, together with microstratigraphic data, will unravel the perimortem history of the FN3-5-MPS individual.

2. The context of Fuente Nueva 3 (FN3)

FN3 is in the north-eastern region of the Guadix-Baza Basin (Granada, Spain) (Fig. 2A and B). FN3 is encompassed in the formerly named Archaeological Zone of the Orce Basin, which also included the site of Barranco León (BL), which has yielded the oldest Western European early hominin remains —a left first deciduous mandibular molar (dm_1) attributed to *Homo* sp. and dated *c.* 1.4 Ma (Oms et al., 2000; Toro-Moyano et al., 2013). In addition, the nearby palaeontological site of Venta Micena (VM) is another key locality for understanding the taphocenosis and paleoecology of the Eurasian Early Pleistocene (e.g. Martínez-Navarro and Palmqvist, 1995; Agustí et al., 2010; Martínez-Navarro et al., 2010).

Discovered in 1991, FN3 is an open-air site with an excavated surface area of 104 m^2, situated in a sedimentary succession deposited at the periphery of the paleo lake Baza. It is located in the Upper Member of the Baza Formation (Fig. 2B–D) (Oms et al., 2011), which is characterized by distal fluvial/alluvial sedimentation (Calvache and Viseras, 1997) and carbonate formations of biogenic and paedogenic origins. Invertebrate fauna associations also record indicate alternating shallow aquatic (ostracod tests of several species, *Bithynia* opercula, etc.), as well as aerial invertebrates (internal shells of *Limax* sp.) (Anadón et al., 2003). The FN3 depositional sequence is divided into seven units, providing three rich archaeo-palaeontological units, denoted FN3-2, FN3-3, and FN3-5.

The age of unit FN3-5 has been dated *c.* 1.2 Ma, using a combination of magnetostratigraphy, biochronology and U-series/ESR methods (Duval et al., 2012). FN3-5 is composed of fine-grained greenish sands and mudstones, and has been further subdivided into subunits 5A and 5B (Fig. 2E; Yravedra et al., 2021). No taphonomic attribute is indicative of re-sedimentation or re-working processes. Excavations in the FN3-5 deposits have additionally provided a number of skeletal remains of large herbivores in anatomical connection, including the proboscidean remains from a single indivudal (FN3-5-MPS).

The faunal assemblage from FN3-5 includes a large variety of large herbivore taxa (Supplementary Table 1), although horses (*Equus altidens*) and mammoths (*M. meridionalis*) are especially well-represented. Mesowear data indicate predominantly browser-dominated diets of

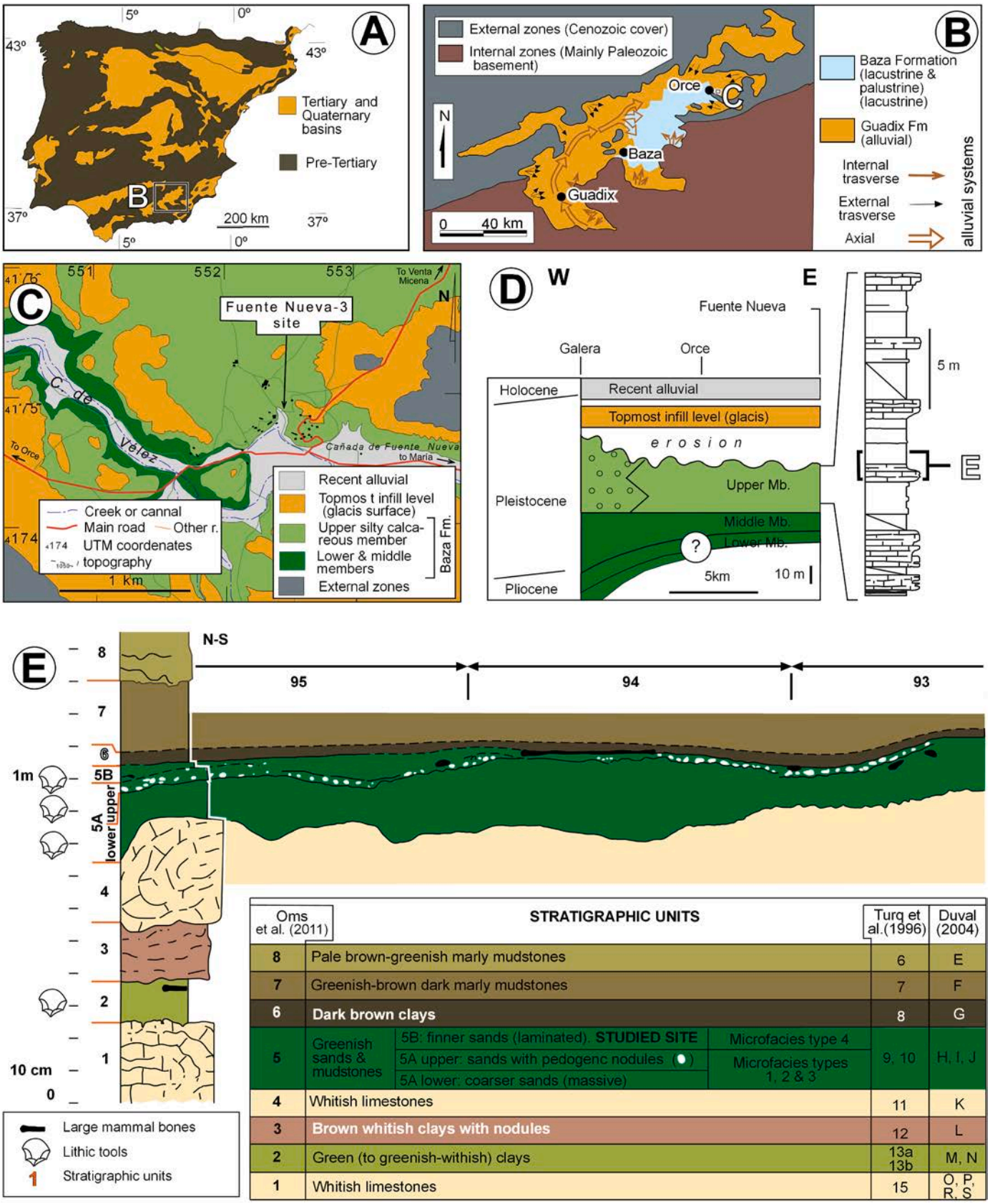

Oms et al. (2011)	STRATIGRAPHIC UNITS			Turq et al.(1996)	Duval (2004)
8	Pale brown-greenish marly mudstones			6	E
7	Greenish-brown dark marly mudstones			7	F
6	**Dark brown clays**			8	G
5	Greenish sands & mudstones	5B: finner sands (laminated). **STUDIED SITE**	Microfacies type 4	9, 10	H, I, J
		5A upper: sands with pedogenc nodules (●)	Microfacies types 1, 2 & 3		
		5A lower: coarser sands (massive)			
4	Whitish limestones			11	K
3	**Brown whitish clays with nodules**			12	L
2	Green (to greenish-withish) clays			13a 13b	M, N
1	Whitish limestones			15	O, P, R, S

Fig. 2. Geographic location and stratigraphic context of the Fuente Nueva 3 site. (A) Location of Fuente Nueva 3 in the Iberian Peninsula. (B) Location of Fuente Nueva 3 in Guadix-Baza Basin. (C) Location of Fuente Nueva 3 at the Archaeological Zone of the Orce Basin. (D) Stratigraphic contextualization of the Fuente Nueva 3 sequence at the Baza Formation. (E) Stratigraphic units of the Fuente Nueva 3 site.

large herbivores (Saarinen et al., 2021). FN3-5 is also abundant in microvertebrates (Supplementary Table 2) which provide important information about the geological age and local environmental conditions. Among the micromammals recovered, *Allophaiomys* aff. *lavocati* and the small-sized variant of *Mimomys savini* stand out, reinforcing a pre-Jaramillo date (Duval et al., 2012). From a palaeoecological point of view, the new genus *Manchenomys orcensis* whose dentition is characterized by hypsodontia (Agustí et al., 2022), indicate relatively dry and cold climate conditions compared with BL: FN3-5 Mean Annual Temperature (MAT): 14.7°; Mean Annual Precipitation (MAP): 618 mm (Sánchez-Bandera et al., 2023).

Pollen analyses of the FN3 units 1–7 (Ochando et al., 2022) depict an environment dominated by open vegetation with pines, junipers, oaks, and wild olive, alongside a diversity of woody taxa including broad-leafed trees, Mediterranean scrub, xerothermic Ibero-north African matorral, chenopods, grasses and mugworts (genus *Artemisia*). A gallery-forest small component is also noticeable in the local vegetation, suggesting the existence of fresh-water bodies, while spores of coprophilous fungi support herbivory by mammals and soil decomposing activity typical of summer-drought regimes.

The FN3 stone tool assemblage is one of the oldest and numerically rich lithic samples representative of the European Oldowan technocomplex (Toro-Moyano et al., 2010, 2011; Barsky et al., 2010, 2015a, 2015b, 2018, 2022). The stone tools have been exhumed in relative abundance from levels FN3-2 and FN3-5 of the site (nearly 1,500 artifacts from excavations 1995–2017, Barsky et al., 2022). Up to now, no significant differences between the toolkits coming from these archaeological units have been noted. On the whole, the assemblage is characterized by an abundance of small-sized flakes made from local flint and limestone (2–3 cm long) and relatively scarce flint cores. Stone reduction operations were carried out mostly *in situ* using both free-hammer and bipolar-on-anvil methods. One of the main features of the assemblage is the differential use of the two raw materials (Barsky et al., 2010) with the flint for flake production, and the limestone blocks and cobbles serving for a wider range of tasks, mainly (but not exclusively) related to percussive activities (e.g. Barsky et al., 2015a). As in other Oldowan assemblages, retouched items are generally very rare and have denticulate morphologies (Barsky et al., 2013); although secondary knapped flakes are present (Zaidner, 2013; Barsky et al., 2015b). While infrequent, some large-sized and loosely configured tools have been identified (e.g. heavy-duty scrapers and chopper-like tools; Barsky et al., 2015a, 2018) (Sup. Table 3).

From a taphonomic point of view, the faunal assemblage of FN3-5 presents a very high degree of fragmentation (Yravedra et al., 2021). The bones found in FN3-5 present generally good preservation rates with low degrees of weathering, alterations produced by water currents, or biochemical processes (Espigares et al., 2019; Yravedra et al., 2021). The impact of carnivores and humans on the fossil assemblage has generally been characterised as being low (Espigares et al., 2019; Yravedra et al., 2021; Palmqvist et al., 2023).

3. Materials and methods

3.1. FN3-5-MPS proboscidean carcass and its individual life history

The analyzed individual is a *M. meridionalis* partial skeleton exhumed at FN3-5 (FN3-5-MPS). To evaluate its life history, biometric data regarding the teeth, pelvis and ribs were used, as provided and published by Ros-Montoya (2010), and then compared with data from other sites (Lister, 1996), specifically, tooth, pelvis and rib measurements.

Pelvic measurements were taken to establish the gender of FN3-5-MPS, with emphasis on the ratio (Gender Index) between the maximum horizontal width of the pelvic aperture (MaxHWPA) and the minimum width of the ilium shaft (MinWIS) (eq. (1)):

$$\text{GenderIndex} = \frac{Max(HWAP)}{Min(WIS)} \quad (1)$$

Further evaluations used to confirm the gender of the individual were performed using a hierarchical clustering algorithm. This was performed based on the ratio of HWPA values of each specimen divided by the largest value of their species (eq. (2)):

$$\text{StandMaxHWPA} = \frac{Max\ (HWPA)_{\text{specimen}}}{Max\ (HWPA)_{\text{largest}}} \quad (2)$$

Age estimates of the individual in African Equivalent Years (AEY) were then carried out by consulting reference data from Laws (1966), Lee et al. (2012) and Stansfield (2015). For dental mesowear analysis, the methodology proposed by Saarinen et al. (2015) was used. Finally, in order to evaluate the gender of FN3-5-MPS in relation with other *M. meridionalis* individuals, a correspondence analysis was conducted using hierarchical clustering algorithm (Ward's method) based on Gender Index and StandMaxHWPA.

3.2. Archaeological soil micromorphology

For the purpose of this part of the study, seven micromorphology samples were extracted from the FN3 Unit 5 sedimentary deposit during data collection in the year 2020, extracting samples from profile Q96-Z96 (Sup. Fig. 1). The samples were collected as undisturbed, oriented blocks using Plaster of Paris bandages. In the lab, they were oven-dried at 50 °C for one day and embedded under vacuum in a mix of polyester resin (Palatal P4-01), polystyrene, and a catalyzer (MEKP). Once hardened, the blocks were sent to Spectrum Petrographics Inc. (Vancouver, USA) to produce large-size petrographic thin sections. The thin sections were observed at Universidad de Jaén using a Zeiss AxioScope 5 polarizing microscope in plane polarized, crossed polarized, oblique incident and ultraviolet light (PPL, XPL, OIL, UV) at magnifications ranging between 20× and 100x. They were also scanned at 50x magnification in plane and crossed polarized light (PPL and XPL), using MWSI Pro Microvisioneer software. For the description and assessment of thin sections, standard guidelines were used (Courty et al., 1989; Stoops, 2003; Goldberg and Macphail, 2006; Macphail and Goldberg, 2010; Nicosia and Stoops, 2017), alongside specialized literature on the microstratigraphy of fluviolacustrine sedimentary environments (Freytet and Plaziat, 1982; Freytet and Verrecchia, 2002; Mallol, 2006, and references therein). For data classification, we used the concept of Microfacies (Courty, 2001; Flügel, 2004).

3.3. Taphonomy

For taphonomic analyses two different methodological approaches were employed for this study, starting with a general and more traditional overview of the taphonomic traces and patterns across the surface of the bones. This analysis was performed using handheld lenses with 10 to 20x magnification, as is common practice (Blumenschine, 1995). General diagnostic criteria defined by Binford (1981) and Domínguez-Rodrigo (2009) were used for the identification of cut marks, whereas tooth and percussion marks were recorded following Blumenschine (1995) and trampling marks were assessed considering the observations by Courtenay et al. (2019a, 2020b). A second, more detailed analysis of bone surface modifications was performed using high resolution 3D modelling of taphonomic traces, geometric morphometrics, and the corresponding classification of marks using Computational Learning (CL).

For the purpose of this study 3D models were constructed using a mixture of Micro-PhotoGrammetry (M-PG, Sup. Fig. 2) and Structured Light Surface Scanning (SLSS, Sup. Fig. 3) (*sensu* Rodríguez-Martín et al., 2015; Maté-González et al., 2017). Use of one technique or the other was dependent on the location of the Region of Interest (ROI), difficulties

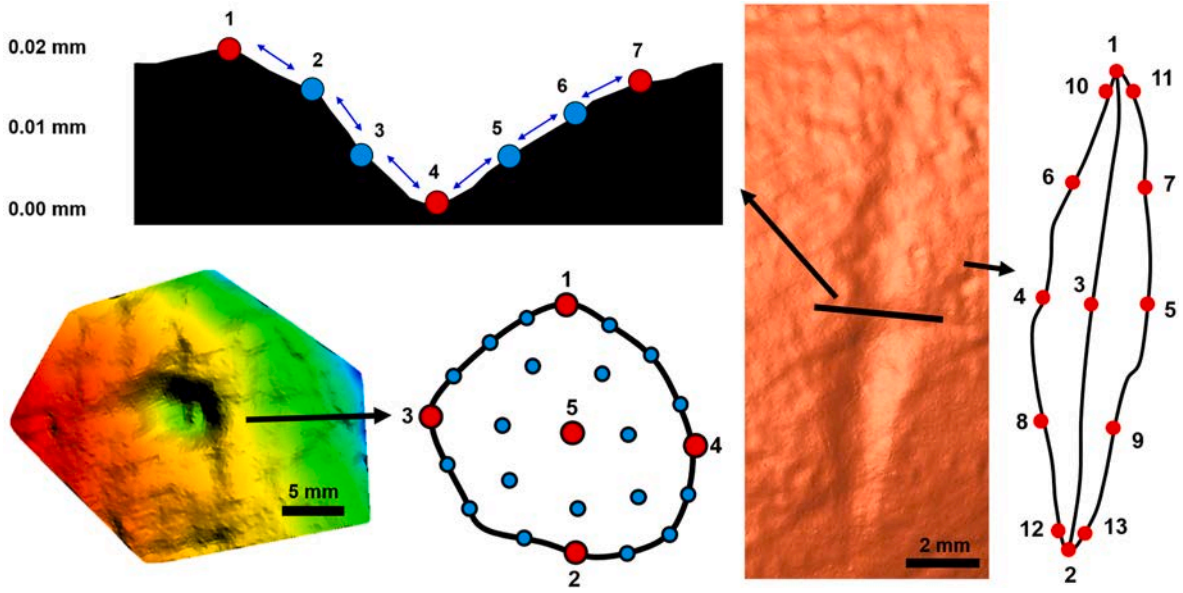

Fig. 3. A presentation of the landmark models used for the purpose of this study, including: (1) the 2D 7-landmark model on linear mark cross-sections, employing the use of 3 fixed landmarks (red) and 4 sliding semi-landmarks (blue); (2) the 3D 13-landmark model for the processing of entire linear mark morphologies; (3) the 3D 25-landmark model for the processing of circular depressions such as percussion and tooth pits.

when manipulating the object under study, as well as any issues produced by the lighting conditions in the museum where FN3-5-MPS is located. Under this premise, documentation of the pelvis was performed via M-PG, while ribs were studied using SLSS. For M-PG a Panasonic Lumix DC-G9 camera was equipped with a 45 mm Leica DG macro lens (45/F2.8; Passive 63 × 62.5 mm sensor). A total of 80 photographs (5184 x 3888 pixels (px); 20.16 Mpx; px size = 12.15 μm) were taken in a single session following a convergent photography method (Sup. Fig. 2) (Rodríguez-Martín et al., 2015), adjusting for the use of natural light in the context of the museum where the photos were taken. For SLSS the DAVID SLS-1 Structured-Light surface scanner of the TIDOP research group (University of Salamanca) was used. This device was calibrated with a 15 mm calibration board and equipped with 52 mm macro lenses to obtain optimal resolution at microscopic scales (Camera = +5, Projector = −10; Sup. Fig. 3).

Depending on the completeness of the mark, two different geometric morphometric models were employed for the processing of linear marks (Fig. 3) (Maté-González et al., 2015; Courtenay et al., 2019b) while a single model was used for the pit (Courtenay et al., 2020b). For cut mark/trampling mark processing, a 3D 13-landmark model was used following Courtenay et al. (2019b), consisting of a landmark configuration using type II and type III landmarks to capture the entire morphology of the trace. When landmark positions were unclear or conditioned by overlapping taphonomic traces, 2D cross-section profiles were extracted from the models to analyze the topography of each trace. For the processing of 2D cross-sections, seven landmarks were used (adapted from Maté-González et al., 2015). Three of these landmarks were of a fixed type, marking the shoulders and deepest-most point of each cross-section. These were followed by two sliding semi-landmarks along each of the walls, amounting to four semi-landmarks in total. The processing of circular traces was performed using a 3D 25-landmark model, also consisting of five type II landmarks, marking the maximum width, length and depth of the pit, followed by a net of semi-landmarks capturing the entire morphology of the pit (Courtenay et al., 2020c). For all configurations, the position of semi-landmarks was optimised by sliding so as to reduce bending energy with a calculated reference specimen (Gunz and Mitteroecker, 2013). For each of the traces, a single experienced individual carried out digitisation procedures.

Each of the archaeological traces was then compared with our extensive experimental samples (Yravedra et al., 2018; Courtenay et al., 2018, 2019a, 2019b, 2020a, 2019b, 2020d, b, 2021). In addition, a sample of experimental cut marks was elaborated by using flint and limestone flakes from local raw materials. Flakes were knapped by right-handed individuals familiar with the knapping strategies observed at the FN3 site. Cut marks were then produced during a butchery experiment using several fleshy articulated pig limbs. Experimental butchery activities produced marks on the bones during defleshing and disarticulation activities. Care was taken to ensure that the flake cutting edges were not affected by attrition. All landmark digitisation procedures were carried out by the same individual.

Statistical analyses and classification tasks were performed in a mixture of the R and Python programming languages. First, landmark coordinates were subjected to a Generalized Procrustes Analysis (GPA), standardizing coordinate data through a series of superimposition procedures involving the translation, rotation and scaling of landmark configurations (Rohlf and Slice, 1990; Bookstein, 1991, *inter alia*). The scaling procedure was either included or excluded depending on the taphonomic traces being analyzed. Under this premise, shape-size information was only included for the analysis of tooth pits. Following this, dimensionality reduction was performed via a Principal Components Analysis, as is common practice in both GM and linear-algebra based data sciences.

Once landmarks had been superimposed, classification tasks of each of the archaeological traces were performed using CL algorithms, following the methods described by Courtenay et al. (2020d, 2021, 2023a). This consists in (1) extracting those Principal Components (PCs) from superimposed components that explain up to 90% of morphological variance, (2) augment the datasets by means of a Markov Chain Monte Carlo (MCMC) algorithm (Gamerman and Lopes, 2006), followed by (3) the training of CL algorithms for classification (Goodfellow et al., 2016). Data augmentation was performed by taking samples and using MCMCs to simulate 100 examples per experimental sample. MCMC performance was evaluated following the suggestions of Courtenay and González-Aguilera (2020a), concluding that the augmented datasets present notable statistical similarities with the original datasets ($|d| = 0.005$, $p < 0.003$). CL algorithms were then trained on these simulated datasets and evaluated using the original data (Courtenay et al., 2023a), noting the prediction loss in the form of Root Mean Squared Error values (RMSE), balanced accuracy, and Kappa (κ) values, to identify whether

algorithms are useful for classification or not. Additionally, sensitivity and specificity results were used to derive Receiver Operating Characteristic curves and their respected Area Under Curve (AUC) values.

CL algorithm architectures adopted those described in Courtenay et al. (2020d) for the 13-landmark model, Courtenay et al. (2021) for the 25-landmark model, while for the 7-landmark model a new algorithm was implemented. This was a simple neural network containing two hidden layers (n = 10 and 8 respectively). No dropout was required, Rectified Linear Unit activation was used for all layers, and the algorithms were trained using the Adam optimization algorithm (Kingma and Ba, 2015). The final activation layer for all algorithms was entirely dependent on whether categorical or binary classification tasks were being performed. Table 1 presents a summary of each of the models' performance obtained for each of the classification tasks.

Finally, algorithms were then used to classify each of the archaeological traces, only using those predictions obtaining over 80% likelihood of being associated to the predicted label as a final result.

4. Results

The tooth belonging to FN3-5-MPS has been identified as a lower last molar (m3), based on morphological and morphometric traits (Sup. Table 4). The straight shape of the lamellae is typical of the genus *Mammuthus*. In addition, the number of lamellae (13) and enamel thickness (3.16 mm) are within the range of *M. meridionalis* (Sup. Table 4; see Ros-Montoya, 2010).

A complete number of lamellae is present but all of them are worn, with the anterior three presenting heavy stages of wear where enamel ridges are still present but have worn down to the bottom of the crown in lateral sides. This stage of m3 wear falls between the age classes of XXV-XXVII of Laws (1966) in African elephant (equivalent of stage L13 of Stansfield (2015) and age class of 48–58.5 years of Lee et al. (2012)). The age of the individual can thus be estimated at roughly 50–60 years in AEY. Mean mesowear angle of the m3 is 102°, indicating a browse-dominated diet (see Saarinen et al., 2015).

The maximum horizontal width (MaxHW) of the pelvic aperture is 1.250 mm, falling between two female *M. meridionalis* individuals from Valdarno (Italy), while male specimens from Valdarno are considerably larger (Lister, 1996). The MinWIS for specimen FN3-5-MPS is 49.4 cm. The Gender Index reaches 2.53. In *M. meridionalis*, this ratio is between 1.63 and 1.95 in the Valdarno male specimens, and between 2.76 and 2.82 in females (Lister, 1996). In *M. trogontherii* these values are normally recorded at *c*. 2–2.21 in males and 2.7–2.9 in females, while in *M. primigenius* values are typically between 1.93 and 2.38 in males (2.64 in a single male specimen) and 2.78–2.86 in females (Lister, 1996).

The Gender Index for FN3-5-MPS falls in between the values for male and female specimens of *M. meridionalis*, with a closer tendency towards those of female individuals. Nevertheless, the comparatively small overall size of the specimen further supports the gender determination as female (Sup. Fig. 4). This is further validated given the results of hierarchical clustering approximating FN3-5-MPS with other female *Mammuthus* specimens based on the Gender Index and StandMaxHWPA values (Sup. Fig. 5).

Finally, the maximum widths of the corpus costae of the two fragmentary rib specimens with modifications (83 mm for FN3-5-MPS-6 and 77 mm for FN3-5-MPS-7) are very similar to the dimensions of anterior ribs of a *M. meridionalis* skeleton (BX 2120) from Rodionovo, Northern Caucasus, which range from 86 mm in the first rib to 76 mm in the sixth rib (Maschenko et al., 2011). Both of these ribs are from the right side of the skeleton. FN-5-MPS-6 is an anterior rib (probably rib nr. 1) slightly dislocated to the side of the skeleton and lying close to the mandible, while FN3-5-MPS-7 is a more posterior one and was found lying on top of the pelvis. It is clear that both of these ribs were dislocated from their original position, making it challenging to determine their original order and position with certainty. Nonetheless, they had stayed in association with the rest of the skeleton and had not been transported away from it.

Table 1
Evaluation results on the trained computational learning algorithms that were used for the classification of taphonomic traces found on the FN3-5-MPS individual. Accuracy, Kappa and Area Under Curve (AUC) values are between 0 and 1, with 1 being the highest obtainable result and values over 0.8 being considered powerful algorithms. Root Mean Squared Error (RMSE) Loss considers values closer to 0 to be indicative of a more accurate model. TM = trampling mark. CM = cut mark.

Classification Tasks	RMSE Loss	Accuracy	Kappa	AUC
7-landmark model (TM vs CM)	0.259	0.90	0.83	0.90
7-landmark Model (raw material)	0.077	0.92	0.86	0.86
7-landmark Model (slice vs cut)	0.018	0.94	0.88	0.93
13-landmark model (TM vs CM)	0.062	0.92	0.83	0.87
13-landmark model (raw material)	0.067	0.95	0.88	0.93
13-landmark model (TM type)	0.101	0.97	0.97	0.93
13-landmark model (slice vs. cut)	0.039	0.94	0.88	0.93
25-landmark model (percussion vs. pit)	0.237	0.96	0.81	0.81
25-landmark model (carnivore taxa)	0.050	0.93	0.86	0.93

4.1. Microstratigraphic and microcontextual analysis of the FN3-5-MPS carcass

Microstratigraphic analyses of FN3-5 (or Level 5) have revealed an inhomogeneous deposit detecting five overlying microfacies units, showing strong differences in composition and sedimentary structure among them (Fig. 4). These microfacies, from bottom to top, are as follows:

Microfacies unit 1 (MF-U1, Level 5A Lower). Paedogenic desiccated mudstone (Fig. 4B): The coarse mineral fraction is composed of medium sand-sized angular quartz grains (50%), sand-to-gravel-sized mammal bone fragments (20%), sand-to-gravel-sized, rounded and subangular marly soil aggregates (10%), silt-to-sand-sized angular opaque mineral grains (5%), ostracod shells (5%), silt-sized muscovite grains (2%), sand-sized avian eggshell fragments (2%) and angular smooth medium gravel-size flint (<2%). The bone remains include spongy bone, cortical bone showing osteons, ivory, medium gravel-size teeth fragments (showing enamel, dentin and cementum) and micrommamal tooth fragments. Spongy and cortical bone fragments show intense cyanobacterial tunnelling and articulated accommodated fractures due to trampling. Also, some bones show a fissured regular pattern due to desiccation. The fine mineral fraction is composed of microsparitic cement. The coarse/fine related distribution is closed-spaced porphyric. Porosity shows straight and skew planes. This microfacies shows a well-developed pedality composed of unaccommodated angular blocky peds. Its microstructure is subangular blocky and the b-fabric is calcitic-crystallitic. This microfacies shows marly soil aggregates containing silt-sized, angular quartz grains (2%) and a micromass composed of micritic calcium carbonate. These aggregates exhibit a fine monic coarse/fine related distribution, a massive microstructure and a calcitic crystallitic b-fabric. They also show localized microsparitic veins and ferruginous mottling.

Microfacies Unit 2 (MF-U2, Level 5A Middle). Massive sand (Fig. 4C): The coarse mineral fraction is composed of fine sand-sized angular quartz grains (50%), silt-sized muscovite grains (10%), silt-sized opaque mineral grains (10%), silt-sized biotite grains (2%), and sand-sized avian eggshell fragments (2%). No fine fraction was observed except for localized clayey lenses and massive clay coatings around mineral grains. The coarse/fine related distribution is monic-chitonic. The microstructure is single-grain and the b-fabric is undifferentiated or granostriated. A few intrapedal, impregnative Fe–Mn oxide orthic nodules were identified. These show a typical morphology and rounded/mammillated internal fabrics. This microfacies unit shows fining-upwards successions of rhythmically bedded sands with reworked bones, ostracods and rounded marly soil aggregates as those described in MF-U1.

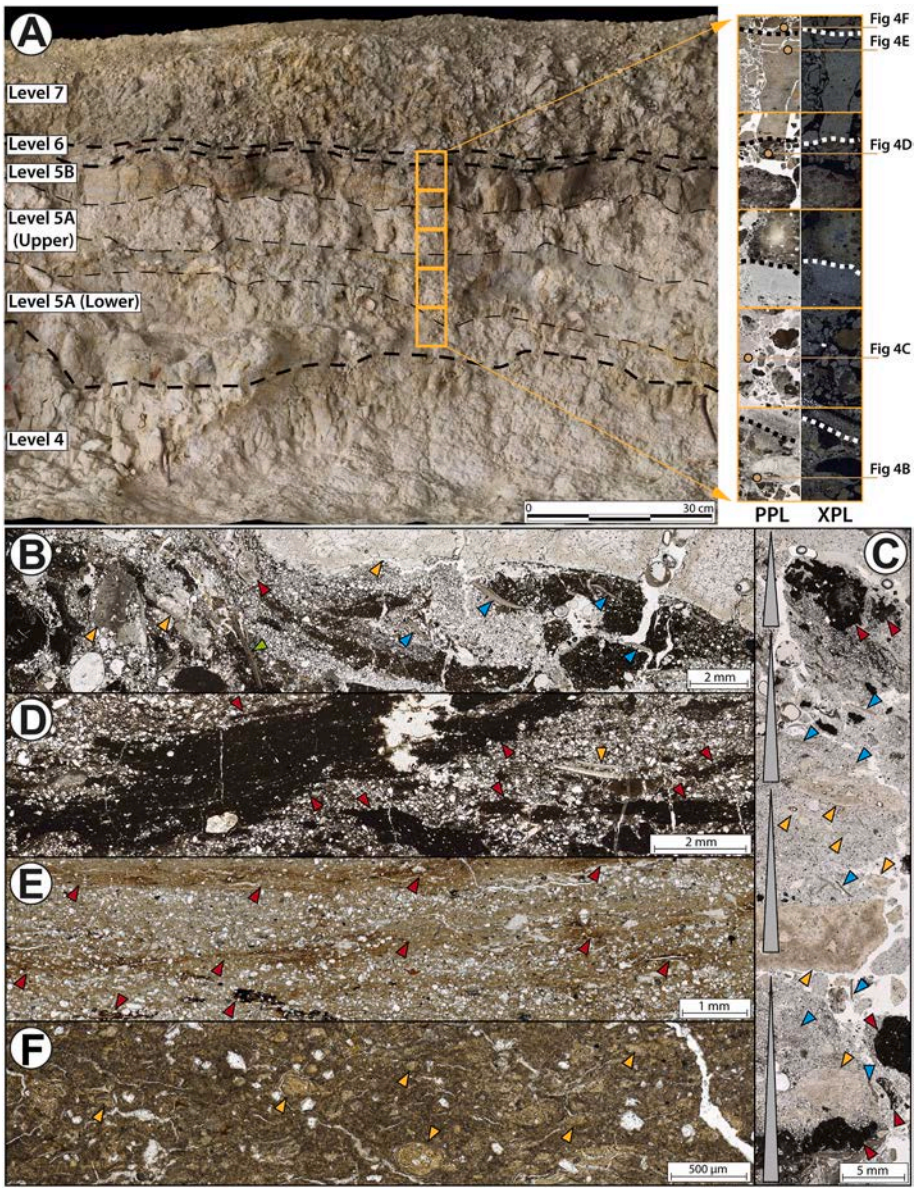

Fig. 4. Microfacies analysis of Level 5: A) Stratigraphic profile Q96-Z96 showing the correlation of the thin sections studied in relation to the site's stratigraphy. B) Level 5A (Lower) - paedogenic desiccated mudstone microfacies (orange arrows: bones; red arrow: microvertebrate tooth; blue arrows: ostracods; green arrow: avian eggshell); C) Level 5A (Upper) - massive sand microfacies (grey triangles: fining-upwards rhythmically bedded fine sand-sized quartz grains; orange arrows: bones; red arrows: soil aggregates; blue arrows: ostracods); D) Level 5A (Upper) - pseudogleyed, cross-bedded silty sand (red arrows: soil aggregates; blue arrows: ostracods); E) Level 5B - pseudogleyed sandy clay (red arrows: Fe–Mn hydromorphic features); F) Level 6 - turbiditic mudstone (orange arrows: ellipsoidal disorthic clay aggregates).

Microfacies Unit 3 (MF-U3, Level 5A Upper). Pseudogleyed cross-bedded silty sand (Fig. 4D): The coarse mineral fraction is composed of medium sand to fine gravel-sized subangular marly soil aggregates (30%) similar to those described in MF-U1, fine sand-sized angular quartz grains (30%), silt-sized muscovite grains (5%), silt-sand-sized angular opaque mineral grains (2%), ostracods (10%) and sand-gravel-sized mammal bone fragments (2%). The fine matrix is composed of microsparitic cement. The coarse/fine related distribution is single-spaced porphyric. The microstructure is massive and the b-fabric is cristallitic. There are intrapedal impregnative Fe–Mn oxide orthic nodules with a typical morphology and rounded/mammillated internal fabrics. Cross-bedding is frequent.

Microfacies Unit 4 (MF-U4, Level 5B Lower). Pseudogleyed sandy clay (Fig. 4E): The coarse mineral fraction is composed of fine sand-sized angular quartz grains (30%), silt-sized muscovite grains (5%), silt-sand-sized angular opaque mineral grains (2%), ostracods (10%) and fine to medium sand-sized reddish orange (PPL) mammal bone fragments (2%). Fine mineral fraction comprises greyish yellow (PPL) to pale gold (XPL) clay. The coarse/fine related distribution is close porphyric. The microstructure is massive and the b-fabric is cross-striated. This microfacies shows hydromorphic features, such as parallel horizontal Fe/Mn linings. Discontinuous, planar, parallel bedding is frequent.

Microfacies Unit 5 (MF-U5, Unit 5B Upper). Turbiditic mudstone (Fig. 4F). The coarse mineral fraction is composed of fine sand-sized angular quartz grains (5%), silt-sand-sized angular opaque mineral grains (2%), and ostracods (10%). Fine mineral fraction comprises greyish brown (PPL) to pale golden grey (XPL) marl. The coarse/fine related distribution is open porphyric. Porosity shows horizontal desiccation cracks. The microstructure is massive and the b-fabric is crystallitic. As pedofeatures, there are abundant fine to coarse sand-sized rounded smooth greyish yellow (PPL) to isotropic (XPL) clay aggregates (30%).

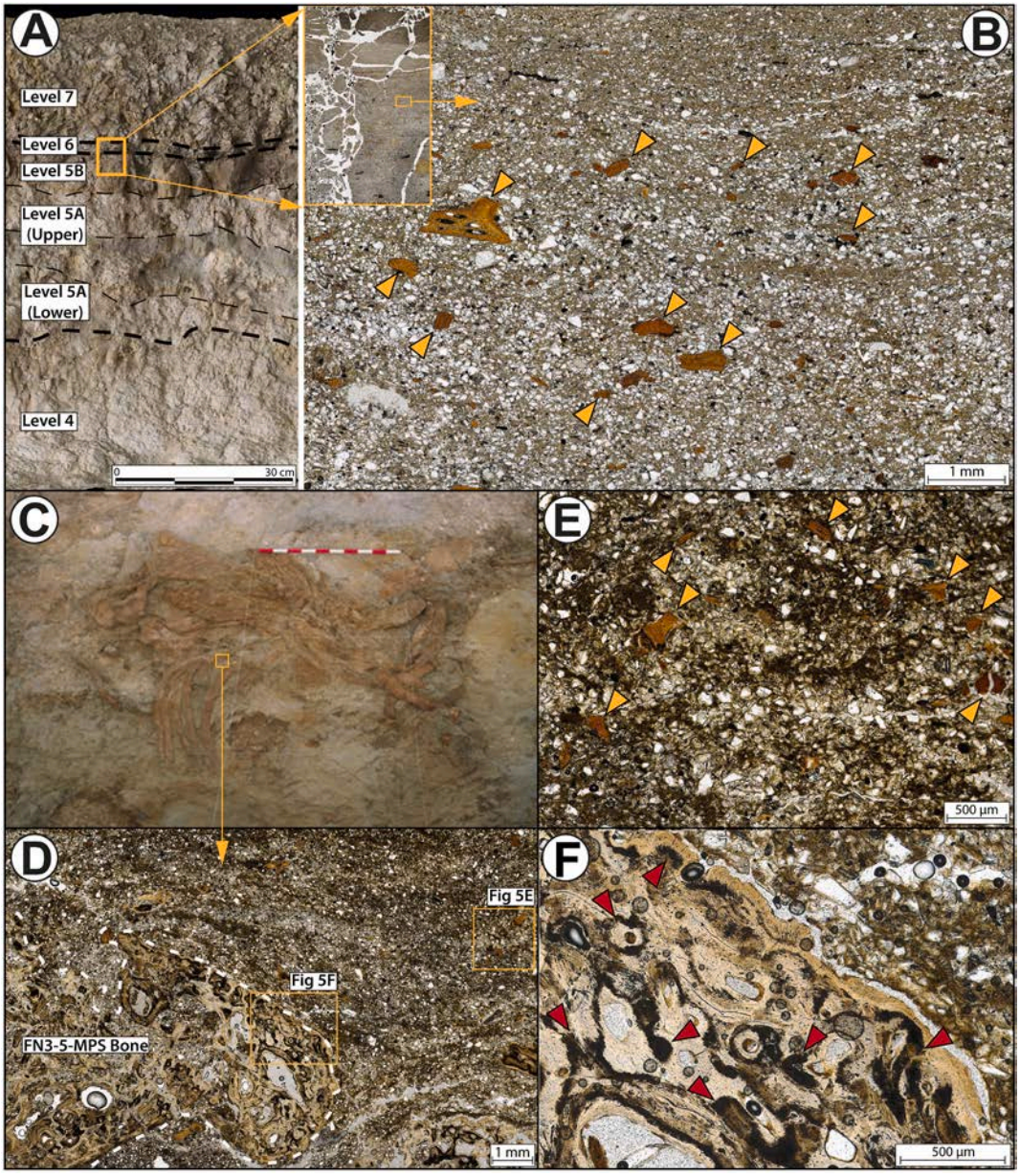

Fig. 5. Microstratigraphic analysis of the FN3-5-MPS remains. A) Stratigraphic profile showing the location of the thin section corresponding to Levels 5b and 6 in relation to the site's stratigraphy. B) Scan of the thin section and microphotograph showing a characteristic water-laid sandy clay sedimentary matrix with discontinuous, wavy, parallel bedding. Note that silt to fine sand-sized reddish-orange (PPL) bones are frequent; C) FN3-5-MPS individual in its sedimentary context. Note that, similarly to Level 5B, the elephant was found within massive greyish-blue clays showing prismatic peds; D) Scan of one of the studied thin sections of the FN3-5-MPS individual's bone (white dotted line) with sediment attached; E) The sedimentary matrix of the FN3-5-MPS individual remains shows discontinuous, wavy, parallel bedding and abundant reddish-orange (PPL) bones, as in Level 5B. F) The FN3-5-MPS individual bones show strong Fe/Mn staining as a result of deposition in water-saturated conditions.

The two thin sections made on the bones of the FN3-5-MPS individual allowed us to identify the original sedimentary matrix in which the *M. meridionalis* laid (Fig. 5A and C). From all the microfacies units described above, the sediment attached to the mammoth bones is similar to MF-U4 pseudogleyed sandy clay (Fig. 5B and D). Thus, the mammoth bones show strong Fe/Mn staining (Fig. 5F), and their sedimentary matrix shows a pseudogleyed sandy clay showing discontinuous, planar, parallel bedding and fine to coarse sand-sized reddish orange (PPL) bones (Fig. 5E).

4.2. Taphonomy of FN3-5-MPS

The FN3-5-MPS individual presents a regularly preserved cortical surface, frequently covered with manganese (Mn) and iron (Fe) oxide staining, with a mixture of both green and dry fractures. Likewise, extensive degrees of biochemical alterations have been noted, alongside a low intensity level of weathering, and low degree of hydraulic alterations.

The *in-visu* examination of preserved cortical surfaces were able to document a total of 22 linear traces on the ventral ($n = 21$) and dorsal ($n = 1$) surfaces of the pelvis (Fig. 6). 19 of them presented highly superficial _/shaped grooves with irregular trajectories. Many were also noted to have discontinuous morphologies with only a few presenting internal microstriations. Only two sets of three of these more superficial marks were observed to present clustering of any type, with one cluster organized in a sub-parallel configuration, and the second cluster

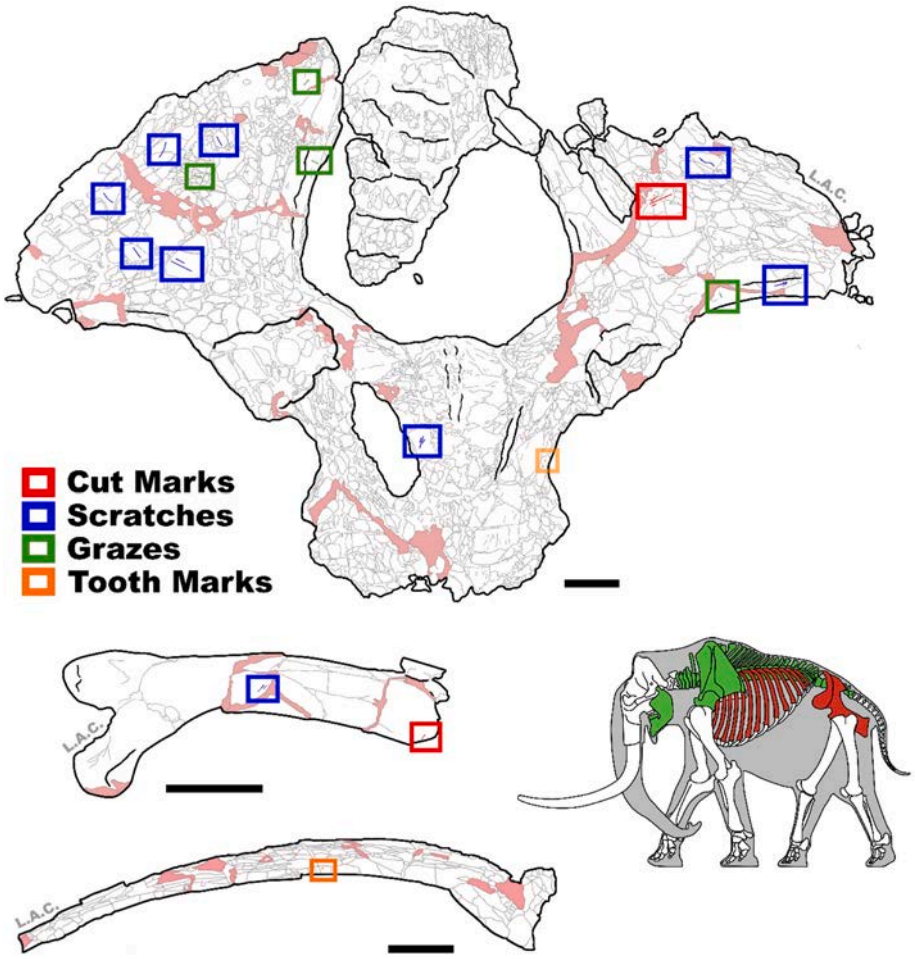

Fig. 6. Taphonomic traces observed and classified on the FN3-5-MPS individual. Areas shaded bright red across the skeleton indicate volumetric reintegrations performed during restoration. Bounding boxes are colour coded according to the trace identified in this area. Semitransparent bounding boxes indicate marks found on the other side of the fossil. Traces are drawn to approximate scale, size of the traces, though may be exaggerated for ease of visualization. Skeletal profile drawing indicates areas with (red) and without (green) taphonomic traces that have been included within this study. Skeletal profile drawing adapted and modified from Larramendi (2016). Scale bars represent 10 cm.

perpendicular and overlapping. All other traces were isolated. Based on these criteria, a total of 19 marks were originally identified as trampling marks.

Three linear traces on the ventral face of the left ilium (Fig. 6) were observed to present a more \/shaped cross section, measuring between 9.82 and 51.13 mm in length, with widths ranging between 0.22 and 0.45 mm, while appearing semi-parallel and grouped among themselves with an oblique orientation. In some areas, a slight degree of shoulder flaking can be observed; however, internal striations are generally absent due to overlaying taphonomic processes. These three traces were originally identified *in-visu* as likely cut marks.

Using high resolution analyses, the three likely cut marks (Fig. 7) were observed to present a more homogeneous morphological trajectory along the mark, while presenting clear, deep \/shaped cross-sections, similar to those observed in cut marks. Analyses additionally confirmed their attribution as cut marks with decision boundaries between ≈96 and 99% probability, while more in-depth analyses were able to associate these marks to simple flint flakes with ≈97% confidence, held at a 90° angle perpendicular to the bone (Table 2).

With regards to the more superficial traces located across the surface of the pelvis, CL algorithms additionally confirmed the original *in-visu* attributions as trampling marks with 88.9–100.0% confidence. Moreover, classification of the type of trampling (Table 3) revealed a predominance of scratches (long and thin marks: $n = 15$) over grazes (short and wide: $n = 4$; *sensu* Courtenay et al., 2019b, 2020d).

Three further linear traces were documented on the dorsal side of the FN3-5-MPS-7 rib, each transversal to the main axis of the bone (Figs. 5 and 6). All three traces present deep grooves with a slightly rounded, yet still \/shaped morphology. Each of the traces are straight without internal striations, nevertheless, original *in visu* characterization of these traces were inconclusive as to whether they could be classified as cut marks or not. Entire morphological analysis of all three marks concluded two of these traces, positioned closer to the articular epiphysis of the rib, to be trampling marks with 99.9 and 100% probability of being scratches (Table 3), while the single trace towards the end of the fragmented bone was classed with 100% probability as being a cut mark produced by flint flakes (Table 2). This singular cut mark is an isolated trace, short and deep, with a \/shaped morphology, very different to the trampling marks located in proximity with the epiphysis of the same bone.

From the perspective of the trampling marks, the final ratio of scratches:grazes observed across both the pelvis and the rib was established at 3:1, proving to be notably analogous with bones trampled on while still being fresh ($\chi^2 = 0.33$, $p = 0.57$) (*sensu* Courtenay et al., 2020c). This coincides with both previous (Espigares et al., 2013), and present interpretations, supported by degrees of weathering, that sedimentation was relatively fast.

Finally, two single circular depressions were observed on the FN3-5-MPS individual. The first on the ventral face of the FN3-5-MPS-7 rib, and the second located on the dorsal ischial body of the pelvis. Both marks

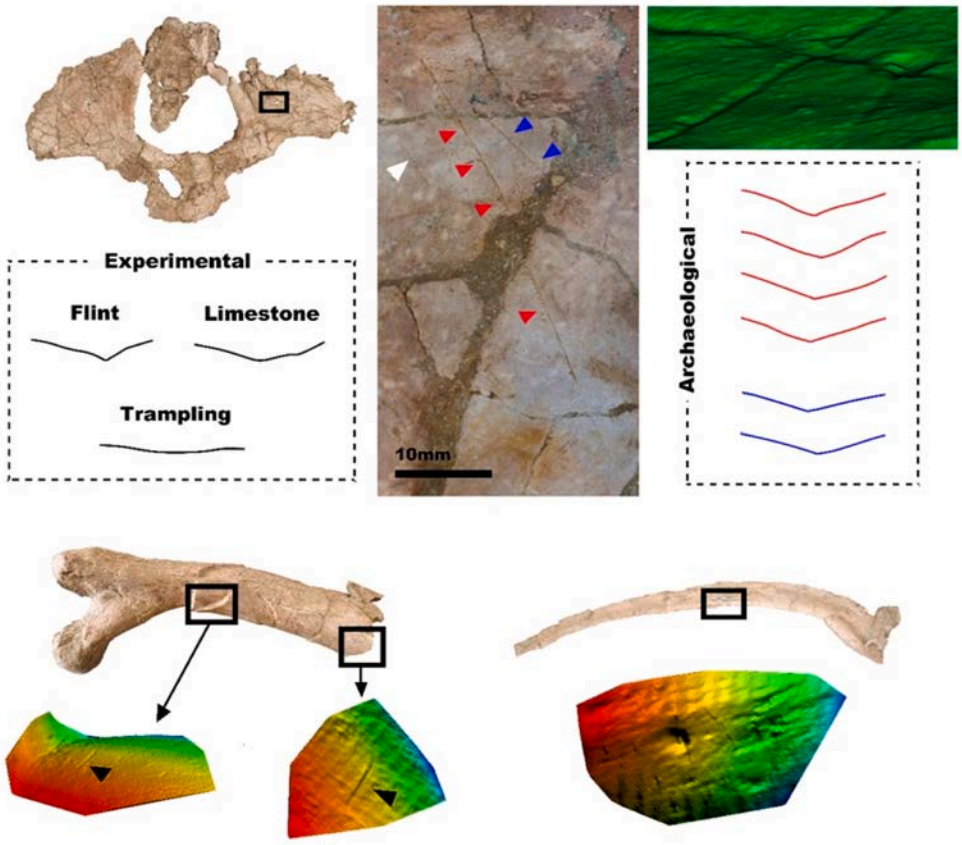

Fig. 7. Documentation of the major taphonomic traces observed on FN3-5-MPS. Upper panels: Cut marks observed on the pelvis, including 3D photogrammetric orthophoto and 2D cross-section profiles derived from 3D models of both experimental comparative samples (right) and real archaeological samples (left). Coloured arrows overlapping the orthophoto correspond to where cross sections were taken with the white arrow indicating a third more superficial cut mark. Bottom panels: 3D models of different traces (trampling mark, cut mark and tooth pit, respectively) and their location on each of the ribs.

Table 2
Probability (Prob.; %) of label association for each of the 4 marks identified on the FN3-5-MPS individual's pelvis and rib. CM = cut mark.

Bone	Prob. CM	Prob. Flint	Prob. 90°
Pelvis	96.68	97.07	100.00
Pelvis	97.57	96.81	100.00
Pelvis	99.76	96.81	100.00
Rib	100.00	96.89	100.00

were classified with a 98% confidence interval of being tooth marks, with final probabilities between a 99.45% and 95.46%, respectively, of having been produced by a large sized feliform individual, close in form to modern day *Panthera leo*.

5. Discussion

According to results obtained in the present paper, the FN3-5-MPS individual has been classified as a *M. meridionalis* female which died at 50–60 years of age. Such an age is indicative that this individual was an old individual approaching the end of its estimated lifespan for a proboscidean of its size. In addition, the diet of this individual must have been mostly browsing, which agrees with inferences for the Venta Micena (VM) and FN3 proboscideans (Saarinen et al. in prep.).

5.1. The depositional genesis of FN3 Level 5 in relation to the environmental context of the FN3-MPS individual

The microstratigraphic analysis of FN3-5 has revealed that, far from being a single homogenous level, this deposit presents strong textural, compositional and diagenetic differences pointing out a complex formation history. The micromorphological sample dataset has shown sedimentary features that provide significant clues about the formation

Table 3
Measurements and classification results of all the trampling marks identified on the FN3-5-MPS proboscidean individual.

Bone	Face	Length (mm)	Width (mm)	Probability (%)	Classification
Pelvis	Dorsal	6.25	0.23	100.0	Scratch
Pelvis	Ventral	4.86	0.33	91.1	Graze
Pelvis	Ventral	5.71	0.05	100.0	Scratch
Pelvis	Ventral	2.39	0.26	94.1	Graze
Pelvis	Ventral	6.09	0.49	94.0	Graze
Pelvis	Ventral	5.48	0.25	100.0	Scratch
Pelvis	Ventral	16.18	0.02	100.0	Scratch
Pelvis	Ventral	6.54	0.26	100.0	Scratch
Pelvis	Ventral	6.91	0.23	100.0	Scratch
Pelvis	Ventral	6.91	0.23	100.0	Scratch
Pelvis	Ventral	4.37	0.21	99.3	Scratch
Pelvis	Ventral	10.29	0.02	100.0	Scratch
Pelvis	Ventral	3.28	0.03	100.0	Scratch
Pelvis	Ventral	4.92	0.11	100.0	Scratch
Pelvis	Ventral	4.41	0.39	94.1	Graze
Pelvis	Ventral	12.26	0.01	100.0	Scratch
Pelvis	Ventral	1.25	0.04	96.9	Scratch
Pelvis	Ventral	1.88	0.05	99.9	Scratch
Pelvis	Ventral	17.15	0.85	100.0	Scratch
Rib	Dorsal	4.99	0.52	94.1	Graze
Rib	Dorsal	3.11	0.25	88.9	Graze

processes of this layer, that are fundamental for the interpretation of site formation processes.

MF-U1 (Level 5A-Lower) exemplifies this complexity; a paedogenic desiccated mudstone showing lacustrine features (presence of ostracods and microsparitic cement), and fluvially-derived floodplain detrital features (quartz sand and reworked marly soil aggregates showing desiccation pores and marmorization patches). These features are characteristic of "desiccation breccia" lake margin facies (Freytet and Verrecchia, 2002), representative of regressive phases during which a deltaic dry mudflat develops on a former lake shore wetland due to aridification entailing abrupt desiccation, erosion and subsequent micro-karstification, or infill of desiccation cracks by sediment input during flash floods or simply rainfall (Platt, 1989; Alonso Zarza et al., 1992; Freytet and Plaziat, 1978). MF-U1 is associated with abundant open-air exposure features, such as mammal bones, microvertebrate teeth and isolated avian eggshell fragments (Canti, 2017), which links the main evidence of megafauna and hominin activity at the site with this kind of seasonally marked environment. Under the microscope, the bone assemblage is taphonomically diverse, including fresh, angular *in situ* broken fragments, together with biodegraded bones indicative of prolonged surface exposure (cracking, cyanobacterial tunneling) (Villagran et al., 2017). This suggests that faunal remains in this layer constitute a palimpsest, formed on a stable mudflat in a deltaic environment. In situ bone breakage could be explained by megafaunal trampling.

MF-U2 (Level 5A-Upper), on the other hand, is composed of well sorted, massive sands. This microfacies unit exhibits fining-upwards successions of rhythmically bedded fine sand-sized quartz with minor amounts of muscovite, opaque minerals, reworked bones, ostracods and rip-up clasts (coming from the underlying microfacies unit) of rounded soil aggregates showing microsparitic cement. This deposit is a characteristic fluviolacustrine microfacies of lake margin fluvial fans in which the mudflat is episodically covered by overbank flow from channel avulsion (Hubert and Hyde, 1982; Miall, 2006). Lacustrine components such as ostracod and bivalve shells are only present in small amounts. The absence of bioturbation points to a fast sedimentation regime. We presume that this is the facies in which previous authors proposed that the individual FN3-5-MPS was deposited (Espigares et al., 2013, 2019; Palmqvist et al., 2023).

MF-U3 is a fluviolacustrine pseudogleyed, cross-bedded silty sand (Level 5A-Upper). It is composed of rounded lacustrine marly soil aggregates showing curved planes and channels with microsparitic hypocoatings formed after plant growth, due to root metabolism (Wieder and Yaalon, 1982). Also, these mudstone aggregates show sparitic laminae after mineralization of biological algal felts. Subsequently, these pores and the mammal bone porosity as well were infilled with microsparitic cement and quartz sand after plant and organic tissue decay. The clast-supported fabric of this deposit, together with the lack of paedogenic features, suggests a rapid rate of fluvially-derived sedimentation. Another lacustrine feature is the presence of ostracods in small amounts. The presence of these features indicates the vicinity of the lake shore and suggests local reworking of lacustrine mudstones in a lake shore colonized by plants and algae.

MF-U4 (Level 5B-Lower), a fluviolacustrine pseudogleyed sandy clay deposit, is well sorted and composed of discontinuous, planar, parallel bedded, fluvially-derived clastic materials, such as clay, silt to fine sand-size subrounded quartz, opaque minerals, and silt-size muscovite. Besides, the widespread presence of ferruginous staining hydromorphic features, (mottling and parallel horizontal linings), in absence of bioturbation and other paedogenic features, is indicative of a permanently or semi-permanently waterlogged, seasonally marked, deltaic floodpain environment with water table fluctuations (Vepraskas et al., 2018). Slight reworking of the lake shore is evidenced in the presence of very few, reworked lacustrine mudstone aggregates. In this microfacies unit, it is important to note the presence of fine to medium sand-sized reddish orange (PPL) mammal bone fragments, transported by water.

Finally, MF-U5 (Level 5B-Upper) is a lacustrine turbiditic mudstone deposit. It is a massive micritic mudstone formed under shallow water, in a low-energy environment below the water base. This deposit shows lacustrine features typical of a lake margin regressive facies, such as ostracods affected by post-mortem short-distance transport and reworking (thanatocoenosis), or the presence of desiccation porosity showing horizontal joint planes and poorly developed curved planes. Finally, rounded to ellipsoidal disorthic clay aggregates are very abundant. These "clay pellets" formed through clay flocculation and aggregate formation due to density differences, followed by turbiditic short-distance transport causing abrasion and rounding and, finally, by settling out in the water column, resulting in deposition. Considered together, these features are indicative of a permanent water column and a calm sedimentation environment in a lake transgressive phase, in which fluvial genesis was brief, as shown in the minor amounts of clastic material (quartz, muscovite and opaque minerals).

Therefore, FN3 represents a distal lake margin, directly influenced by fluvial fan sedimentation. Comparable palustrine facies associated with early hominin occupation have been documented at 'Ubeidiya, Israel (e.g. Unit II22f, Mallol, 2006). Accordingly, taking all the microfacies units together in their stratigraphic succession, FN3-5 represents a shift from a regressive (MF-U1 to MF-U4) to a transgressive phase (MF-U5) within the Baza paleolake dynamic. FN3-5 provides therefore evidence of fluviolacustrine environments with a stable dry mudflat at the base (MF-U1) that developed into a deltaic floodplain subjected to flash floods (MF-U2), a lake shore colonized by plants and algae (MF-U3), and a permanently or semi-permanently waterlogged deltaic floodplain with water table fluctuations (MF-U4).

Finally, FN3-5 shows a lacustrine genesis at the top in turbiditic conditions (MF-U5). During this time span, animals, including hominins, frequented the lake shore recurrently, during a regressive phase of alternating wet (marsh) and dry (mudflat) landscapes resulting from seasonal shifts in precipitation. Sedimentation during this period was also seasonal, linked with abrupt fluvial input (sandy overbank flow) after rainfall episodes. While similar observations had been previously reported (Duval et al., 2010), we disagree with the recurrently stated hypothesis of FM3-5 representing a single season in which a lacustrine submerged setting dried up, was occupied by hominins and other animals, and later buried by fluvial sands (Yravedra et al., 2021). This hypothesis contradicts our micromorphological evidence of paedogenesis, hydromorphic features and palimpsest bone assemblage formation.

One of the animals that frequented the lake shore was the FN3-5-MPS individual. The thin sections performed in its bones and their attached sediment indicate that this mammoth died during the deposition of the MF-U4 (Level 5B-Lower), the pseudogleyed sandy clay. Thus, the mammoth bones are included in a water-laid sandy clay sedimentary matrix showing discontinuous, wavy, parallel bedding, in which silt to fine sand-sized reddish orange (PPL) bones are frequent. The mammoth bone shows strong Fe/Mn staining because of its deposition in water saturation conditions, suggesting that the mammoth died in a waterbody and its carcass remained underwater (MF-U4). These observations made at the microscale coincide with the graphic record available from the excavation of the proboscidean (Espigares et al., 2013). Looking carefully at the images provided by Espigares et al. (2013), it can be appreciated that the *M. meridionalis* was found in massive greyish-blue clays showing prismatic peds, which are compatible with MF-U4 (Level 5B).

Considering our microstratigraphic analysis and reinterpretation of the available graphic record, we disagree with previous interpretations regarding the association of the proboscidean carcass with both the archaeological artifacts and their geological context. Specifically, with the published association of FN3-5-MPS with "a thick layer of fine sands, which were deposited in a short sedimentary event" (Espigares et al., 2013: 115). Thus, our observations on the textural complexity and composition of the sedimentary matrix of FN3-5-MPS become relevant, since the sedimentary environment in which this individual died would

not be a lake margin as proposed by Espigares et al. (2013: Fig. 7) in their graphic reconstruction, but a permanently or semi-permanently waterlogged deltaic floodplain with water table fluctuations. Considering this observation, together with the microstratigraphic complexity of FN3-5, the association of the carcass with 34 coprolites and 17 lithic artifacts would be an example of the risks of the 'Pompeii premise' (Ascher, 1961; Binford, 1981; Schiffer, 1985).

Such a case can also be found at the Barogali site (Republic of Djibouti) where 569 artifacts were found around an almost complete skeleton of *P. recki* without any direct evidence of human activity, cut or anthropic fracture marks (Chavaillon et al., 1986; Berthelet and Chavaillon, 2001; Berthelet, 2002).

Given these limits, direct evidence on the bones (e.g. tooth and cut marks, and/or green fractures) is needed to determine if the carcass was consumed by hominins and animals, and in what conditions, as shown below.

5.2. Tooth marks and cut marks on the FN3-5-MPS proboscidean individual

New results obtained from the FN3-5-MPS individual, derived through a combination of 3D modelling, geometric morphometrics and computational learning, have revealed the intervention of both hominins and carnivores on this fossil.

Beginning with the possible interventions of carnivores, the current data reveal a high probability of associating the tooth pits identified with those produced by large felids, such as *Homotherium*, *Megantereon,* and *Panthera*. The former must, however, be ruled out considering the single species of *Panthera* likely to be contemporaneous with this landscape (*P.* cf. *gombaszoegensis*) is a closer analogy with modern *P. onca* (Turner and Antón, 1997), which was not found to be a likely match to the morphological features of these pits. From this perspective, and considering the result that the morphological affinities of the FN3-5-MPS, the tooth pits seem more related with modern *P. leo*, thus they can be more likely attributed to this tooth damage to a large machairodontine. This is not surprising given that in nearby localities of Orce (VM3 and BL) a handful of bones with the presence of tooth marks, likely attributable to machairodontines, have also been detected (Yravedra et al., 2022; Courtenay et al., 2023). In addition, other sites such as Friesenhahn Cave (USA) (Marean and Ehrhardt, 1995), Olduvai (Tanzania) (Domínguez Rodrigo et al., 2007), Rancho La Brea (USA) (De Santis et al., 2012) and Haile 21A (USA) (Domínguez-Rodrigo et al., 2022) have provided evidence to support the capacity of saber-toothed felids to produce alterations to bone cortical surfaces.

Such a recurrence could be indicative that bone modifications by machairodontines are apparently common. Additionally, this refutes the repeated idea that macariodontines cannot leave tooth marks due to their high craniodental specialization (e.g. Martínez-Navarro and Palmqvist, 1995, 1996; Palmqvist et al., 2007, 2023; Espigares et al., 2013). This does not imply their intent to process hard tissues (e.g. fracture to access bone marrow), but the consequence of accidently biting when processing the soft tissues close to the bone (see discussion in Courtenay et al., 2023).

From a different perspective, previous research has generally proposed *Pachycrocuta brevirostris* as the main carnivore to have intervened in the formation of FN3. In particular, this taxon has been characterized as a specialist in breaking bones to access marrow (Arribas and Palmqvist, 1998; Palmqvist et al., 2011). The association of *P. brevirostris* with the FN3-5-MPS individual has been proposed based on the presence of coprolites found in proximity of the carcass (Espigares et al., 2013, 2019; Palmqvist et al., 2023). Typical hyenid activity on extant megafaunal carcasses, such as proboscideans, usually produce some degree of furrowing to the edges of pelves, ribs, vertebral apophysis (Crader, 1983; Haynes and Klimowicz, 2015; Haynes, 2017), scapulae and appendicular bones (Haynes, 2017; Haynes et al., 2020b). Furrowing has been also recorded on extinct proboscidean bones (Yravedra et al., 2010; Mangano and Bonfiglio, 2012). However, and in spite of the presence of 14 ribs, 18 vertebrae, the pelvis, one of the scapulae and the mandible of this individual, such modifications are completely absent from FN3-5-MPS. While recent research by Palmqvist et al. (2023) ponder the notion that *P. brevirostris* would have carefully selected certain bones for bone-cracking activities, so as to avoid dislocating their jaws, this is evidently open to debate, given the evolution of bone-cracking adaptations in these species (Ferretti, 2007), and the bone-cracking abilities of modern hyenids when processing megafaunal carcasses (*ibid.*).

On the other hand, our study suggests that the cut marks on the bones were likely produced by simple flint flakes. Apart from the discrepancy in the number of pieces of lithic industry between the publication of Espigares et al. (2013) and Palmqvist et al. (2023), we examined 15 of the items claimed to be in relation with the FN3-5-MPS individual (Museo Arqueológico de Granada, Fig. 8). Five of which are made from limestone (FN3.02.V94-50215; FN3.02.S95-50218; FN3.02.T95-40; FN3.02.S96-7; FN3.03.S96-23), and so unlikely to be related with the cut marks. Two pieces (FN3.03.T96-21; FN3.03.T96-41) are flint fragments. All of them were found in the Upper level, according to bibliography, except for one limestone debris which lacks any stratigraphic ascription (FN3.03.T96-41).

The production of cut marks using simple, small, unmodified flint flakes, such as those observed in the FN3 Level 5 lithic assemblage (Toro-Moyano et al., 2011), is consistent with the experimental analyses of Starkovich et al. (2021), who considered this type of stone tools to be particularly useful for defleshing megafaunal carcasses, while larger flakes are more suited for dismemberment. These authors do not indicate the dimensions of such larger flakes, while it is also important to point out that only three of the flint flakes in this assemblage (FN3.03.U94-8; FN3.02.R95-1; FN3.03.T96) are >40 mm long.

The presence of cut marks in the ventral area of the pelvis indicates that hominins had access to the carcass very early. This is especially noteworthy given that carnivorans typically access proboscidean carcasses through soft tissues such as the underbelly, genitalia, and anus (Haynes, 1988, 2006, 2017; White and Diedrich, 2012; Haynes and Klimowicz, 2015). The location of these cut marks on the cranio-ventral (anterior) surface of the left iliac wing, at the attachment surface for the iliacus muscle, could indicate cutting of the iliopsoas (iliacus + psoas) muscles. This could be associated with several different butchery activities, such as the removal of guts from the abdominal cavity, similar to observations by Duffy (1984) of hunter-gatherer populations accessing the intestinal contents when first coming across a carcass. The presence of both cut marks and tooth marks on the pelvis, however, present an interesting conundrum regarding the first agent to access the carcass. The most probable scenario considers felids to have expelled the hominins, or vice versa. Another possibility is that either the hominins or the felids had already satisfied their hunger and/or that the hominins had processed the parts for their transportation in a sequential manner (Fig. 9). Regardless, it is plausible to suggest that both had very early access to FN3-5-MPS.

The taphonomic history of this individual becomes even more interesting when we consider the presence of both cut and felid tooth marks on two ribs. The cut marks on the ribs are likely associated with the cutting through intercostal muscles, and perhaps an attempt to open the ribcage to reach muscles and organs in the thoracic cavity. The documented carnivore damage, on the other hand, is more indicative of access to internal organs and softer tissues. A plausible scenario to explain the anatomical proximity of the cut and tooth marks would be conditioned by the large amount of food provided by a carcass of a *M. meridionalis* individual. Thus, the availability of muscle packages and viscera would allow for at least two different taxa, humans and saber-tooth felids, to have had access to parts of FN3-5-MPS.

Finally, some authors have claimed that the limbs were removed and transported by humans based on the simple absence of the limbs (Espigares et al., 2013, 2019; Palmqvist et al., 2023). However, even the

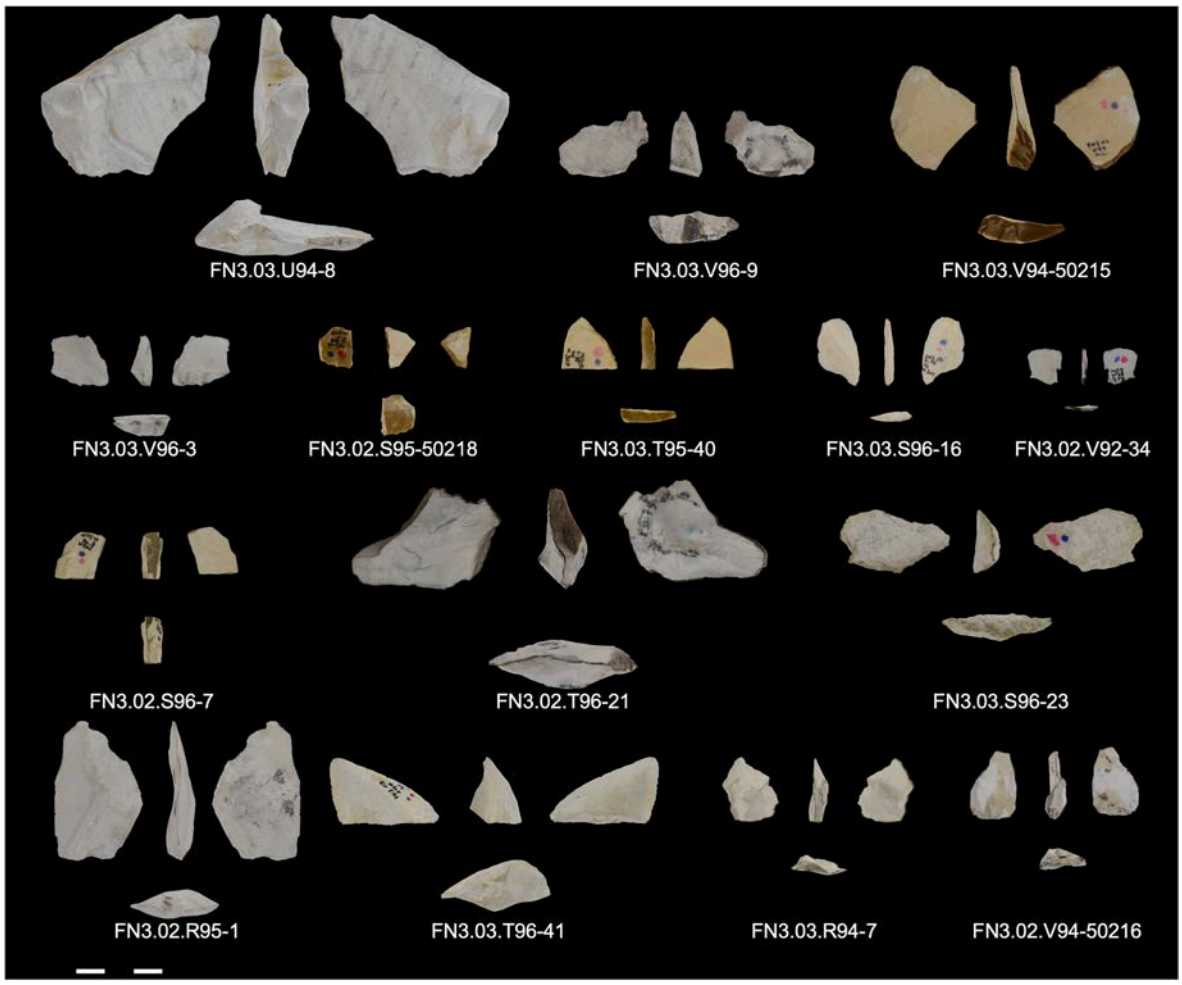

Fig. 8. The lithic artifacts indicated in the Museo Arqueológico de Granada as being in spatial association with the FN3-5-MPS carcass. Scale = 3 cm. Photo: María Higueras.

evidence presented in this study for the exact position of the cut marks on the pelvic girdle are insufficient to state that humans dismembered and transported any of the limbs of FN3-5-MPS. It is important to note that ethnographic records demonstrating the removal of elephant bones often involve the use of metal knives and axes (Duffy, 1984; Haynes, 1987, 1991; Haynes and Klimowicz, 2015). Therefore, drawing a direct analogy between early European populations using the ~2–~2.5 cm flint flakes observed at FN3 (Barsky et al., 2010), and modern hunter-gatherers equipped with metal tools, is not necessarily feasible. Additionally, many different agents could be responsible for these missing limbs, including carnivores as well as other mammoths themselves (Haynes, 1988; Haynes et al., 2020b). Finally, we cannot discard the possibility of discovering the limbs in future excavations.

In the light of these observations, three main points can be raised in response to those proposed by Palmqvist et al. (2023). First, regarding the lack of marks due to the thickness of periosteum, we have proved that marks are indeed present, therefore a thick periosteum is not a significant factor. Second, as has been debated in other research (Courtenay et al., 2023), the delicate dentition of machairodontine felids is not sufficient to prove that they *cannot* leave marks on bone, just that they are *less likely* to. Finally, Palmqvist et al. (2023) state that the absence of marks is due to poor preservation conditions during the three years in which the excavation of FN3-5-MPS took place. This final point does not consider the protective measures that were taken by the conservation and restoration team, and supervised by technicians of the Regional Government of Andalusia, to prevent this from damaging the fossils. Needless to say, the present study is proof that marks are indeed observable on these remains, providing highly notable insights into the taphonomic history of this individual.

6. Conclusions

In the light of the results presented in this study we can draw the following conclusions:

1. Microstratigraphy has shown a complex sequence of stratigraphic facies throughout FN3-5, providing evidence to support the FN3-5-MPS individual to have died in the MF-U4 facie. Any association of said partial skeleton with materials deposited in other Level 5 sublevels or microfacies is therefore spurious, specifically with those from the level of greenish sands (MF-U2) referred to as Level 5 (or Upper Archaeological Level) in previous works (Espigares et al., 2013; Palmqvist et al., 2023).
2. Cut and tooth marks have been found on the cortical surface of some of the FN3-5-MPS bones, proving the access of both hominins and carnivores to this carcass. The former would have most likely used flint flakes to process this carcass, while the latter are highly likely to have been machairodontine felids.
3. Although hyenids usually leave many marks on megafaunal remains, no evidence of furrowing or hyenid tooth marks have been identified here.
4. The location of the cut marks on the pelvis and one of the ribs may reflect human processing activities of the right hindlimb and intercostal muscles. The position of tooth marks on the ilium and another

Fig. 9. Recreation of the exploitation of FN3-5-MPS by hominins (top) and machairodontines (bottom). Artwork: Jesús Gamarra.

rib, however, indicate that machairodontines worked in areas very similar to humans. In light of this, it can be assumed that both groups had early access to the carcass. Based on the available data, however, we cannot determine which of them intervened first. Regardless, we can state that their access to the carcass must have been swift and occurred prior to it being submerged in water.

5. Despite the coincidence in the intervention areas of humans and machairodontines, we have no proof of direct competition between both taxa.
6. The anthropogenic alterations observed on the FN3-5-MPS bones make FN3 part of the select group, along with Dmanisi (Tappen et al., 2022) and La Boella (Mosquera et al., 2015; Pineda et al., 2017), of localities from the Early Pleistocene with evidence of human processing of proboscidean carcasses in Eurasia.
7. Finally, this paper shows how an interdisciplinary approach, combining taphonomy, micromorphology, stratigraphy, and palaeontology, can shed a detailed light on particular stories. In this case, the death and processing of the carcass of a female mammoth in what is now the Early Pleistocene site of FN3 (Orce, Granada, Spain).

Author contributions

J.Y. – Conceptualization, Validation, Investigation, Resources, Data curation, Writing – original draft preparation, Supervision, Funding acquisition; L.A.C. – Conceptualization, Methodology, Software, Validation, Formal analysis, Investigation, Resources, Data curation, Writing – original draft, review and editing, Visualization.; M.G.R. – Conceptualization, Methodology, Formal analysis, Investigation, Writing – original draft preparation, Visualization; J.F.R.-G. – Investigation, Resources, Visualization; J.S. – Conceptualization, Methodology, Investigation, Writing – original draft preparation, review and editing; N.E. – Conceptualization, Methodology, Formal analysis, Investigation, Writing – original draft preparation, Visualization; C.L. – Investigation, Resources, Data curation, Writing – review & editing; J.J.R.-A. – Investigation, Resources, Data curation; J.S. – Investigation, Resources, Data curation; E.M.-J. – Investigation, Resources, Data curation; J.C.-D. – Investigation, Resources, Data curation; D.H.-R. – Investigation, Resources, Data curation; V.E. – Investigation, Resources, Data curation; A. S.-R. – Investigation, Resources, Data curation; G.A.-S. – Investigation, Resources, Data curation; H.B. – Investigation, Resources, Data curation; D.DM. – Investigation, Resources, Data curation; A.F. – Investigation, Resources, Data curation; J.G. – Resources, Data curation, Visualization; A.G.-A. – Investigation, Resources, Data curation; J.J.G.Q. – Investigation, Resources, Data curation; F.J-E. – Investigation, Resources, Data curation; A.K. – Investigation, Resources, Data curation; M.M. – Investigation, Resources, Data curation; J.O. – Investigation, Resources, Data curation; P.P. – Investigation, Resources, Data curation; C.S.-B. – Investigation, Resources, Data curation; S.V.-K. – Investigation, Resources, Data curation; M.F. – Investigation, Resources, Data curation, Supervision, Funding acquisition; J.A. – Investigation, Resources, Data

curation, Supervision, Funding acquisition; H.-A.B. – Investigation, Resources, Data curation, Supervision, Funding acquisition; J.C. – Investigation, Resources, Data curation, Supervision, Funding acquisition; D. B. – Investigation, Resources, Data curation, review and editing, Supervision, Funding acquisition; C.M. – Conceptualization, Methodology, Formal analysis, Investigation, Writing – original draft preparation, Visualization; J.M.J.-A. – Conceptualization, Investigation, Resources, Data curation, Writing – original draft preparation, review and editing, Visualization, Supervision, Project administration, Funding acquisition.

Declaration of competing interest

The authors declare that they have no known competing financial interests or personal relationships that could have appeared to influence the work reported in this paper.

Data availability

Data will be made available on request.

Acknowledgements

Research at Fuente Nueva 3 is currently possible thanks to the support and approval of the Consejería de Turismo, Cultura y Deporte (Junta de Andalucía, Spain) through the General Research Project (2023–2026) Evolución humana y paleoecología a partir de los yacimientos pleistocenos de la Zona Arqueológica 'Cuenca de Orce'. Retos y desafíos (Ref: SIDPH/DI/MCM).

This research has been carried out thanks to projects PID 2021.125098NB.I00 funding by MCIN/AEI/10.13039/501100011033/FEDER Una manera de hacer Europa and ProyExcel_00274 funding by Dirección General de Planificación de la Investigación (Consejería de Universidad, Investigación e Innovación, Junta de Andalucía). In addition, this research has been supported by the following projects of the Spanish government: PID2021-122533NB-I00, PID2021-123092NB-C21, PID2022-136832NB-I00. We also acknowledge the support provided by the PALARQ Foundation through the project Ref: PR2004_19/01.

The research of C.S·B., D.B., P·P., S.T., J.A., and H.-A.B. is funded by the CERCA Programme/Generalitat de Catalunya. A.F.M. was supported by an APOST postdoctoral grant (APOST/2021/110, Generalitat Valenciana) cofinanced by the European Social Fund, and is currently supported by a Margarita Salas contract from the Ayudas para la recualificación del sistema universitario español (MS21-048), Ministerio de Universidades del Gobierno de España, financed by the European Union-NextGenerationEU. S.T is supported by a Margarita Salas employment contract for access to the Spanish System of Science, Technology, and Innovation at the Universitat Rovira i Virgili (2021URV-MS-03) funded by the European Union-NextGenerationEU, the Ministry of Universities and the Recovery, Transformation and Resilience Plan. P.P is supported by a Juan de la Cierva - Incorporación contract (grant IJC2020-044108-I) funded by MCIN/AEI/10.13039/501100011033 and "European Union-NextGenerationEU/PRTR". Similiarly, we also have to acknowledge the financial support provided by the PALARQ Foundation, funded through the project titled "Dilucidando la acción de los carnívoros en los yacimientos del Pleistoceno Inferior Ibérico del Pontón de la Oliva (Madrid) y de Fuente Nueva 3 y de Venta Micena 3 y 4 (Granada). Ref: PR2004_19/01". The work of J.S. was funded by the Academy of Finland during this work (AoF. project nr. 340775/346292, NEPA - Non-analogue ecosystems in the past).

Additionally, we wish to acknowledge the support provided by Isidro Toro-Moyano Director of the Archaeological Museum of Granada until 2022 and María Higueras for her help in the elaboration of Figs. 1 and 8. We would also like to thank Santiago Borragán from the Cabárceno Park for providing access to some referential materials. Also to Marcia Ponce de León and Christoph Zollikofer for their comments on earlier versions of the manuscript which helped to improve the final version. In addition, we would like to acknowledge the two reviewers who have contributed to the improvement the previous version of this paper. Last but not least, we would like to thank the team that excavated skeleton FN3-5-MPS from 2001 to 2003.

Appendix A. Supplementary data

Supplementary data to this article can be found online at https://doi.org/10.1016/j.quascirev.2024.108561.

References

Agam, A., Barkai, R., 2018. Elephant and mammoth hunting during the Paleolithic: a review of the relevant archaeological, ethnographic and ethno-historical records. Quaternary 1 (1), 3. https://doi.org/10.3390/quat1010003.

Aguilera-Gamboa, E., 1913. Torralba, la plus ancienne station humaine de l'Europe?. In: Congrés International du Anthropologie et d'Archeologie Préhistoriques (Geneve 1912). Compte Rendu. XIV, Session, pp. 277–290.

Agustí, J., Blain, H.A., Furió, M., De Marfá, R., Santos-Cubedo, A., 2010. The Early Pleistocene small vertebrate succession from the Orce region (Guadix-Baza Basin, SE Spain) and its bearing on the first human occupation of Europe. Quat. Int. 223–224, 162–169. https://doi.org/10.1016/j.quaint.2009.12.011.

Agustí, J., Piñero, P., Lozano-Fernández, I., Jiménez-Arenas, J.M., 2022. A new genus and species of arvicolid rodent (Mammalia) from the Early Pleistocene of Spain. Comptes Rendus Palevol 21, 847–858. https://doi.org/10.5852/cr-palevol2022v21a39.

Alonso Zarza, A.M., Calvo, J.P., García del Cura, M.A., 1992. Palustrine sedimentation and associated features—grainification and Pseudo-Microkarst—in the Middle miocene (intermediate unit) of the Madrid basin, Spain. Sediment. Geol. 76 (1), 43–61. https://doi.org/10.1016/0037-0738(92)90138-H.

Anadón, P., Julià, R., Oms, O., 2003. Estratigrafía y estudio sedimentológico preliminar de diversos afloramientos en Barranco León y Fuente Nueva (Orce, Granada). In: Toro, I., Agustí, J., Martínez-Navarro, B. (Eds.), El Pleistoceno inferior de Barranco León y Fuente Nueva 3, Orce (Granada). Memoria científica Campañas 1999-2002, Monografías de Arqueología, vol. 17, pp. 47–72 (Junta de Andalucía. Consejería de Cultura, 2003).

Arribas, A., Palmqvist, P., 1998. Taphonomy and palaeoecology of an assemblage of large mammals: hyaenid activity in the lower Pleistocene site at Venta Micena (Orce, Guadix-Baza Basin, Granada, Spain). Geobios 31, 3–47. https://doi.org/10.1016/S0016-6995(98)80056-9.

Ascher, R., 1961. Analogy in archaeological interpretation. SW. J. Anthropol. 17, 317–325.

Barsky, D., Celiberti, V., Cauche, D., Grégoire, S., Lebègue, F., Lumley, H., Toro-Moyano, I., 2010. Raw material discernment and technological aspects of the Barranco León and Fuente Nueva 3 stone assemblages (Orce southern Spain). Quat. Int. 223–224, 201–219. https://doi.org/10.1016/j.quaint.2009.12.004.

Barsky, D., Garcia, J., Martínez, K., Sala, R., Zaidner, Y., Carbonell, E., Toro-Moyano, I., 2013. Flake modification in European Early and Early-Middle Pleistocene stone tool assemblages. Quat. Int. 316, 140–154. https://doi.org/10.1016/j.quaint.2013.05.024.

Barsky, D., Vergès, J.M., Sala, R., Menéndez, L., Toro-Moyano, I., 2015a. Limestone percussion tools from the late early Pleistocene sites of Barranco León and Fuente Nueva 3 (Orce, Spain). Philos. Trans. R. Soc. B 370, 20140352. https://doi.org/10.1098/rstb.2014.0352.

Barsky, D., Sala, R., Menéndez, L., Toro-Moyano, I., 2015b. Use and re-use: Re-knapped flakes from the mode 1 site of Fuente Nueva 3 (Orce, Andalucía, Spain). Quat. Int. 361, 21–33. https://doi.org/10.1016/j.quaint.2014.01.048.

Barsky, D., Vergès, J.M., Titton, S., Guardiola, M., Sala, R., Toro-Moyano, I., 2018. The emergence and significance of heavy-duty scrapers in ancient stone toolkits. Comptes Rendus Palevol 17 (3), 201–219. https://doi.org/10.1016/j.crpv.2017.09.002.

Barsky, D., Titton, S., Sala-Ramos, R., Bargalló, A., Grégoire, S., Saos, T., Serrano-Ramos, A., Oms, O., Solano-García, J.A., Toro-Moyano, I., Jiménez-Arenas, J.M., 2022. The significance of subtlety: contrasting lithic raw materials procurement and use patterns at the Oldowan sites of Barranco León and Fuente Nueva 3 (Orce, Andalusia, Spain). Front. Earth Sci. 2022, 10. https://doi:10.3389/feart.2022.893776.

Berthelet, A., Chavaillon, J., 2001. The early palaeolithic butchery site of Barogali (Republic of Djibuti). In: Cavarretta, G., Gioia, P., Mussi, M., Palombo, M.R. (Eds.), Proceedings of the 1st International Congress the World of Elephants. Consiglio Nazionale delle Ricerche, Roma, pp. 176–179.

Berthelet, A., 2002. Barogali et l'Oued Doure. Deuz gisements représentatifs du Paléolithique ancien en République de Djibouti. L'Anthropologie 106, 1–39. https://doi.org/10.1016/S0003-5521(02)01087-7.

Binford, L.R., 1981. Bones: Ancient Men and Modern Myths. Academic Press, New York.

Blumenschine, R.J., 1995. Percussion marks, tooth marks and the experimental determinations of the timing of hominid and carnivore access to long bones at FLK Zinjanthropus, Olduvai Gorge, Tanzania. J. Hum. Evol. 29, 21–51. https://doi.org/10.1006/jhev.1995.1046.

Bookstein, F., 1991. Morphometric Tools for Landmark Data: Geometry and Biology. Cambridge University Press, New York.

Calvache, M.L., Viseras, C., 1997. Long-term control mechanisms of stream piracy processes in southeast Spain. Earth Surf. Process. Landforms 22, 93–105. https://doi.org/10.1002/(SICI)1096-9837(199702)22:2<93::AID-ESP673>3.0.CO;2-W.
Canti, M.G., 2017. Avian eggshell. In: Nicosia, C., Stoops, G. (Eds.), Archaeological Soil and Sediment Micromorphology. John Wiley & Sons, Ltd, pp. 39–41. https://doi.org/10.1002/9781118941065.ch2.
Chavaillon, J., Guérin, C., Boisaubert, J.-L., Coppens, Y., 1986. Découverte d'un site de dépeçage à Elephas recki, en République de Djibouti. Comptes Rendus de l'Académie des Sciences - Series II 302, 243–246.
Chazan, M., Horwitz, L.K., 2006. Finding the message in intricacy: the association of lithics and fauna on lower paleolithic multiple carcass sites. J. Anthropol. Archaeol. 25 (4), 436–447. https://doi.org/10.1016/j.jaa.2006.03.005.
Courtenay, L.A., Maté-González, M.Á., Aramendi, J., Yravedra, J., González-Aguilera, D., Domínguez-Rodrigo, M., 2018. Testing accuracy in 2D and 3D geometric morphometric methods for cut mark identification and classification. PeerJ 6, e5133. https://doi.org/10.7717/peerj.5133.
Courtenay, L.A., Yravedra, J., Huguet, R., Ollé, A., Aramendi, J., Maté-González, M.Á., González-Aguilera, D., 2019a. New taphonomic advances in 3D digital microscopy: a morphological characterization of trampling marks. Quat. Int. 517, 55–66. https://doi.org/10.1016/j.quaint.2018.12.019.
Courtenay, L.A., Yravedra, J., Maté-González, M.Á., Aramendi, J., González-Aguilera, D., 2019b. 3D analysis of cut marks using a new geometric morphometric methodological approach. Archaeol. Anthropol. Sci. 11, 651–665. https://doi:10.1007/s12520-017-0554-x.
Courtenay, L.A., González-Aguilera, D., 2020a. Geometric morphometric data augmentation using generative computational learning algorithms. Appl. Sci. 10, 9133. https://doi.org/10.3390/app10249133.
Courtenay, L.A., Huguet, R., Yravedra, J., 2020b. Scratches and grazes: a detailed microscopic analysis of trampling phenomena. J. Microsc. 277 (2), 107–117. https://doi.org/10.1111/jmi.12873.
Courtenay, L.A., Herranz-Rodrigo, D., Huguet, R., Maté-González, M.Á., González-Aguilera, D., Yravedra, J., 2020c. Obtaining new resolutions in carnivore tooth pit morphological analyses: a methodological update for digital taphonomy. PLoS One 15 (10), e0240328. https://doi.org/10.1371/journal.pone.0240328.
Courtenay, L.A., Huguet, R., González-Aguilera, D., Yravedra, J., 2020d. A hybrid geometric morphometric Deep learning approach for cut and trampling mark classification. Appl. Sci. 10, 150. https://doi10.3390/app10010150.
Courtenay, L.A., Herranz-Rodrigo, D., González-Aguilera, D., Yravedra, J., 2021. Developments in data science solutions for carnivore tooth pit classification. Sci. Rep. 11, 10209 https://doi.org/10.1038/s41598-021-89518-4.
Courtenay, L.A., Aramendi, J., González-Aguilera, D., 2023a. Recruiting a skeleton crew – methods for simulating and augmenting paleoanthropological data using Monte Carlo based algorithms. Am. J. Biol. Anthropol. 181 (3), 1–20. https://doi.org/10.1002/ajpa.24754.
Courtenay, L.A., Yravedra, J., Herranz-Rodrigo, D., Rodríguez-Alba, J.J., Serrano-Ramos, A., Estaca-Gómez, V., González-Aguilera, D., Solano, J.A., Jiménez-Arenas, J. M., 2023b. Deciphering carnivoran competition for animal resources at the 1.46 Ma early Pleistocene site of Barranco León (Orce, Granada, Spain). Quat. Sci. Rev. 300, 107912 https://doi.org/10.1016/j.quascirev.2022.107912.
Courty, M.A., 2001. Microfacies analysis assisting archaeological stratigraphy. In: Goldberg, P., Holliday, V.T., Ferring, C.R. (Eds.), Earth Sciences and Archaeology. Springer US, Boston, MA, pp. 205–239.
Courty, M.A., Macphail, R.I., Goldberg, P., 1989. Soils and Micromorphology in Archaeology, Cambridge Manuals in Archaeology. Cambridge University Press, Cambridge.
Crader, D.C., 1983. Recent single-carcass bone scatters and the problem of "butchery" sites in the archaeological record. In: Clutton-Brock, J., Grigson, C. (Eds.), Animals and Archaeology. Vol. 1. Hunters and Their Prey, vol. 163. BAR International Series, Oxford, pp. 107–141.
Delagnes, A., Lenoble, A., Harmand, S., Brugal, J.P., Prat, S., Tiercelin, J.J., Roche, H., 2006. Interpreting pachyderm single carcass sites in the African Lower and Early Middle Pleistocene record: a multidisciplinary approach to the site of Nadung'a 4 (Kenya). J. Anthropol. Archaeol. 25, 448–460. https://doi.org/10.1016/j.jaa.2006.03.002.
de la Torre, I., Albert, R.M., Arroyo, A., Macphail, R., McHenry, L.J., Mora, R., Njau, J.K., Pante, M.C., Rivera-Rondón, C.A., Rodríguez-Cintas, A., Stanistreet, I.G., Stollhofen, H., Wehr, K., 2018. New excavations at the HWK EE site: archaeology, paleoenvironment and site formation processes during late Oldowan times at Olduvai Gorge, Tanzania. J. Hum. Evol. 120, 140–202. https://doi.org/10.1016/j.jhevol.2017.07.018.
De Santis, L.R.G., Schubert, B.W., Scott, J.R., Ungar, P.S., 2012. Implications of diet for the extinction of saber-toothed cats and American lions. PLoS One 7, e52453. https://doi.org/10.1371/journal.pone.0052453.
Domínguez-Rodrigo, M., Barba, R., Egeland, C.P., 2007. Deconstructing Olduvai: A Taphonomic Study of the Bed I Sites. Springer, Dordrecht.
Domínguez-Rodrigo, M., Juana, S., Galán, A.B., Rodríguez, M., 2009. A new protocol to differentiate trampling marks from butchery marks. J. Archaeol. Sci. 36, 2643–2654. https://doi.org/10.1016/j.jas.2009.07.017.
Domínguez-Rodrigo, M., Bunn, H.T., Mabulla, A.Z.P., Baquedano, E., Uribelarrea, D., Pérez-González, A., Gidna, A., Yravedra, J., Díez-Martín, F., Egeland, C., Barba, R., Arriaza, M.C., Organista, E., Ansón, M., 2014. On meat eating and human evolution: a taphonomic analysis of BK4b (Upper Bed II, Olduvai Gorge, Tanzania), and its bearing on hominin megafaunal consumption. Quat. Int. 322–323, 129–152. https://doi.org/10.1016/j.quaint.2013.08.015.
Domínguez-Rodrigo, M., Egeland, C.P., Cobo-Sanchez, L., Baquedano, E., Hulbert Jr., R. C., 2022. Sabertooth carcass consumption behavior and the dynamics of Pleistocene large carnivoran guilds. Sci. Rep. 12 (1), 6045. https://doi.org/10.1038/s41598-022-09480-7.
Duffy, K., 1984. Children of the Forest. Dodd, Mead, and Co., New York.
Duval, M., Toro Moyano, I., Falguères, C., Mestour, B., Perrenoud, C., Espigares Ortiz, M. P., Ros Montoya, S., 2010. Lithostratigraphic study of the Town Hall of Fuente Nueva 3 (Orce, Guadix-Baza Basin, Spain). In: Martínez Navarro, B., Agustí i Ballester, J., Toro Moyano, I. (Eds.), Human Occupations in the Lower and Middle Pleistocene of the Guadix-Baza Basin. Ministry of Culture, pp. 57–76.
Duval, M., Falguères, C., Bahain, J.-J., Grün, R., Shao, Q., Aubert, M., Dolo, J.M., Agustí, J., Martínez-Navarro, B., Palmqvist, P., Toro-Moyano, I., 2012. On the limits of using combined U-series/ESR method to date fossil teeth from two Early Pleistocene archaeological sites of the Orce area (Guadix-Baza basin, Spain). Quat. Res. 77 (3), 482–491. https://doi.org/10.1016/j.yqres.2012.01.003.
Espigares, M.P., Martínez-Navarro, B., Palmqvist, P., Ros-Montoya, S., Toro, I., Agustí, J., Sala, R., 2013. *Homo* vs. *Pachycrocuta*: earliest evidence of competition for an elephant carcass between scavengers at Fuente Nueva-3 (Orce, Spain). Quat. Int. 295, 113–125. https://doi.org/10.1016/j.quaint.2012.09.032.
Espigares, M.P., Palmqvist, P., Guerra-Merchán, A., Ros-Montoya, S., García-Aguilar, J. M., Rodríguez-Gómez, G., Serrano, F.J., Martínez-Navarro, B., 2019. The earliest cut marks of Europe: a discussion on hominin subsistence patterns in the Orce sites (Baza basin, SE Spain). Sci. Rep. 9, 15408 https://doi.org/10.1038/s41598-019-51957-5.
Espigares, M.P., Palmqvist, P., Rodríguez-Ruiz, M.D., Ros-Montoya, S., Pérez-Ramos, A., Rodríguez-Gómez, G., Guerra-Merchán, A., García-Aguilar, J.M., Granados, A., Campaña, I., Martínez-Navarro, B., 2023. Sharing food with hyenas: a latrine of *Pachycrocuta brevirostris* in the early Pleistocene assemblage of Fuente Nueva-3 (Orce, Baza Basin, SE Spain). Archaeol. Anthropol. Sci. 15, 81. https://doi.org/10.1007/s12520-023-01784-7.
Ferretti, M.P., 2007. Evolution of bone-cracking adaptations in hyaenids (Mammalia, Carnivora). Swiss J. Geosci. 100, 41–52.
Flügel, E., 2004. Microfacies of Carbonate Rocks: Analysis, Interpretation and Application. Springer-Verlag, Berlin, Heidelberg.
Freeman, L.G., Butzer, K.W., 1966. The Acheulian station of Torralba (Spain): a progress report. Quaternaria 8, 9–22.
Freeman, L.G., Howell, F.C., 1981. Acheulian occupation at Ambrona (Spain). In: 46th Annual SAA Meetings Abstract. San Diego.
Freytet, P., Plaziat, J.C., 1978. Le Pseudomicrokarst pédologique: a particular aspect of the paléopédogénèses développées sur les dépôts calcaires lacustres dans le tertiaire du languedoc. In: M, Matter Sturm, A., R, C. (Eds.), Acad. Sci. Paris, vol. 286, pp. 1661–1664.
Freytet, P., Plaziat, J.C., 1982. Continental carbonate sedimentation and pedogenesis-late cretaceous and early tertiary of southern France. In: Contributions to Sedimentology, vol. 12. E. Schweizerbart, Stuttgart.
Freytet, P., Verrecchia, E.P., 2002. Lacustrine and palustrine carbonate petrography: an overview. J. Paleolimnol. 27, 221–237. https://doi.org/10.1023/A:1014263722766.
Gamerman, D., Lopes, H.F., 2006. Markov Chain Monte Carlo. Chapman and Hall, Boca Raton.
Gaudzinski-Windheuser, S., Kindler, L., MacDonald, K., Roebroeks, W., 2023. Hunting and processing of straight-tusked elephants 125.000 years ago: implications for Neanderthal behavior. Sci. Adv. 9, eadd8186 https://doi.org/10.1126/sciadv.add8186.
Goodfellow, I., Bengio, Courville, A., 2016. Deep Learning. MIT Press, Cambridge.
Goldberg, P., Macphail, R.I., 2006. Practical and Theoretical Geoarchaeology. John Wiley & Sons.
Gunz, P., Mitteroecker, P., 2013. Semilandmarks: a method for quantifying curves and surfaces, Hystrix. Italian Journal of Mammalogy 24, 103–109.
Haynes, G., 1987. Elephant-butchering at modern mass-kill sites in Africa. Curr. Res. Pleistocene 4, 75–77.
Haynes, G., 1988. Longitudinal studies of frican elephant death and bone deposits. J. Archaeol. Sci. 15, 131–157. https://doi.org/10.1016/0305-4403(88)90003-9.
Haynes, G., 1991. Mammoths, Mastodonts, and Elephants: Biology, Behavior and the Fossil Record. Cambridge University Press, Cambridge.
Haynes, G., 2006. Mammoth landscapes: good country for hunter-gatherers. Quat. Int. 142–143, 20–29. https://doi.org/10.1016/j.quaint.2005.03.002.
Haynes, G., 2017. Taphonomy of the Inglewood mammoth (*Mammuthus columbi*) (Maryland, USA): green-bone fracturing of fossil bones. Quat. Int. 445 (25), 171–183. https://doi.org/10.1016/j.quaint.2016.02.034.
Haynes, G., 2022. Late quaternary proboscidean sites in Africa and Eurasia with possible or probable evidence for hominin involvement. Quaternary 5 (1), 18. https://doi.org/10.3390/quat5010018.
Haynes, G., Krasinski, K., Wojtal, P., 2020a. A study of fractured proboscidean B 1 ones in recent and fossil assemblages. J. Archaeol. Method Theor 28, 956–1025. https://doi.org/10.1007/s10816-020-09486-3.
Haynes, G., Krasinski, K., Wojtal, P., 2020b. Elephant bone breakage and surface marks made by trampling elephants: implications for interpretations of marked and broken mammoth spp.bones. J. Archaeol. Sci. Rep. 33, 102491 https://doi.org/10.1016/j.jasrep.2020.102491.
Haynes, G., Klimowicz, J., 2015. Recent elephant-carcass utilization as a basis for interpreting mammoth exploitation. Quat. Int. 359–360, 19–37. https://doi.org/10.1016/j.quaint.2013.12.040.
Howell, F.C., 1966. Observations on the earlier phases of the European lower paleolithic. Am. Anthropol. 68, 88–201.
Howell, F.C., Freeman, L.G., 1982. Ambrona: an early stone age site on Spanish Meseta. L. S. B. Leukey Found. News 22 (1), 11–13.

Howell, F.C., Freeman, F.C., 1983. Ivory points from the earlier acheulean of the Spanish meseta. In: Homenaje Al Profesor Martin Almagro Basch. Ministerio de Cultura, Madrid, pp. 41–61.

Hubert, J.F., Hyde, M.G., 1982. Sheet-flow deposits of graded beds and mudstones on an alluvial sandflat-playa System: upper triassic blomidon redbeds, St Mary's Bay, Nova Scotia. Sedimentology 29 (4), 457–474. https://doi.org/10.1111/j.1365-3091.1982.tb01730.x.

Isaac, G.L., Crader, D.C., 1981. To what extent were early hominids carnivorous? An archaeological perspective. In: Harding, R.S.O., Teleki, G. (Eds.), Omnivorous Primates: Gathering and Hunting in Human Evolution. Columbia University Press, New York, pp. 37–103.

Kingma, D.P., Ba, J.L., 2015. Adam: a method for stochastic optimization. In: Proceedings of the 3rd International Conference for Learning Representations. Available from: arXiv: https://arxiv.org/pdf/1412.6980.pdf. (Accessed 11 October 2023).

Larramendi, A., 2016. Shoulder height, body mass, and shape of proboscideans. Acta Palaeontol. Pol. 61 (3), 537–574. https://doi.org/10.4202/app.00136.2014.

Laws, R.M., 1966. Age criteria for the African elephant. East Afr. Wildl. J. 4, 1–37. https://doi.org/10.1111/j.1365-2028.1966.tb00878.x.

Lee, P.C., Sayialel, S., Lindsay, W.K., Moss, C.J., 2012. African elephant age determination from teeth: validation from known individuals. Afr. J. Ecol. 50, 9–20. https://doi.org/10.1111/j.1365-2028.2011.01286.x.

Linares-Matás, G., Yravedra, J., 2021. We hunt to share': social dynamics and very large mammal butchery during the Oldowan–Acheulean transition. World Archaeol. 53, 224–254. https://doi.org/10.1080/00438243.2022.2030793.

Lister, A.M., 1996. Sexual dimorphism in the mammoth pelvis: an aid to gender determination. In: Shoshani, J., Tassy, P. (Eds.), The Proboscidea: Trends in Evolution and Paleoecology. Oxford Science Publications, Oxford, pp. 254–259.

Macphail, R.I., Goldberg, P., 2010. Archaeological materials. In: Stoops, G., Marcelino, V., Mees, F. (Eds.), Interpretation of Micromorphological Features of Soils and Regoliths. Elsevier, Amsterdam, pp. 589–622.

Mallol, C., 2006. What's in a beach? Soil micromorphology of sediments from the Lower Paleolithic site of 'Ubeidiya, Israel. J. Hum. Evol. 51, 185–206. https://doi.org/10.1016/j.jhevol.2006.03.002.

Mangano, G., Bonfiglio, L., 2012. First finding of a partially articulated elephant skeleton from a late Pleistocene hyena den in sicily (san Teodoro Cave, north eastern Sicily, Italy). Quat. Int. 276–277, 53–60. https://doi.org/10.1016/j.quaint.2011.08.034.

Marean, C.W., Ehrhardt, C.L., 1995. Paleoanthropological and paleoecological implications of the taphonomy of a sabertooth's den. J. Hum. Evol. 29, 515–547. https://doi.org/10.1006/jhev.1995.1074.

Martínez-Navarro, B., Palmqvist, P., 1995. Presence of the African machairodont *Megantereon whitei* (Broom, 1937) (Felidae, Carnivora, Mammalia) in the lower Pleistocene site of Venta Micena (Orce, Granada, Spain), with some considerations on the origin, evolution and dispersal of the genus. J. Archaeol. Sci. 22, 569–582. https://doi.org/10.1006/jasc.1994.0054.

Martínez-Navarro, B., Palmqvist, P., 1996. Presence of the African sabertoothed felid *Megantereon whitei* (Broom, 1937) (Mammalia, Carnivora, Machairodontinae) in Apollonia-1 (Migdonia basin, Macedonia, Greece). J. Archaeol. Sci. 23, 869–872. https://doi.org/10.1006/jasc.1996.0081.

Martínez-Navarro, B., Palmqvist, P., Madurell, J., Ros-Montoya, S., Espigares, M.P., Torregrosa, V., Perez-Claros, J.A., 2010. La fauna de grandes mamíferos de Fuente Nueva-3 y Barranco León-5: estado de la cuestión. In: Toro, I., Martínez-Navarro, B., Agustí, J. (Eds.), Ocupaciones Humanas en el Pleistoceno Inferior y Medio de la cuenca de Guadix-Baza. Consejería de Cultura, Sevilla, pp. 197–236.

Maschenko, E.N., Schvyreva, A.K., Kalmykov, N.P., 2011. The second complete skeleton of *Archidiskodon meridionalis* (Elephantidae, Proboscidea) from the stavropol region, Russia. Quat. Sci. Rev. 30, 2273–2288. https://doi.org/10.1016/j.quascirev.2011.06.003.

Maté-González, M.Á., Yravedra, J., González Aguilera, D., Palomeque, J., Domínguez-Rodrigo, M., 2015. Micro-photogrammetric characterization of cut marks on bones. J. Archaeol. Sci. 62, 128. https://doi.org/10.1016/j.jas.2015.08.006, 14.

Maté-González, M.Á., Aramendi, J., González-Aguilera, D., Yravedra, J., 2017. Statistical comparison between low-cost methods for 3D characterization of cut-marks on bones. Rem. Sens. 9 (9), 873. https://doi.org/10.3390/rs9090873.

Miall, A.D., 2006. The geology of fluvial deposits. Sedimentary facies, basin analysis, and petroleum geology, fourth ed. Springer Verlag, Berlin, Heidelberg.

Monahan, C.M., 1996. New zooarchaeological data from bed II, Olduvai Gorge, Tanzania, implications for hominid behaviour in the early Pleistocene. J. Hum. Evol. 31, 93–128. https://doi.org/10.1006/jhev.1996.0053.

Mosquera, M., Saladié, P., Ollé, A., Cáceres, I., Huguet, R., Villalaín, J.J., Carrancho, Á., Bourlès, D., Braucher, R., Vallverdú, J., 2015. Barranc de la Boella (Catalonia, Spain): an acheulean elephant butchering site from the European late early Pleistocene. J. Quat. Sci. 30, 651–666. https://doi.org/10.1002/jqs.2800.

Nicosia, C., Stoops, G., 2017. Archaeological Soil and Sediment Micromorphology. John Wiley & Sons, Ltd.

Oms, O., Parés, J.M., Martínez-Navarro, B., Agustí, J., 2000. Early human occupation of Western Europe: paleomagnetic dates for two paleolithic sites in Spain. Proc. Natl. Acad. Sci. USA 97, 10666–10670. https://doi.org/10.1073/pnas.180319797.

Oms, O., Anadón, P., Agustí, J., Julià, R., 2011. Geology and chronology of the continental Pleistocene archeological and paleontological sites of the Orce area (Baza Basin, Spain). Quat. Int. 243 (1), 33–43. https://doi.org/10.1016/j.quaint.2011.03.048.

Ochando, J., Carrión, J., Altolaguirre, Y., Munuera, M., Amorós, G., Jiménez-Moreno, G., Solano-García, J., Barsky, D., Luzón, C., Sánchez-Bandera, C., Serrano-Ramos, A., Toro-Moyano, I., Saarinen, J., Blain, H.-A., Bocherens, H., Oms, O., Agustí, J., Fortelius, M., Jiménez-Arenas, J.M., 2022. Palynological investigations in the Orce archaeological Zone, early Pleistocene of southern Spain. Rev. Palaeobot. Palynol. 304, 10472 https://doi.org/10.1016/j.revpalbo.2022.104725.

Palmqvist, P., Martínez-Navarro, B., Pérez-Claros, J.A., Torregrosa, V., Figueirido, B., Jiménez-Arenas, J.M., Patrocinio-Espigares, M., Ros-Montoya, S., De Renzi, M., 2011. The giant hyena Pachycrocuta brevirostris: modeling the bone-cracking behavior of an extinct carnivore. Quat. Int. 243, 61–79. https://doi.org/10.1016/j.quaint.2010.12.035.

Palmqvist, P., Rodríguez-Gómez, G., Martínez-Navarro, B., Espigares, M., P Figueirido, B., Ros-Montoya, S., Guerra-Merchan, A., Granados, A., García-Aguilar, J. Ma, Pérez-Claros, J.A., 2023. Déjà vu: on the use of meat resources by sabretooth cats, hominins, and hyaenas in the Early Pleistocene site of Fuente Nueva 3 (Guadix-Baza Depression, SE Spain). Archaeological and Anthropological Sciences 15, 17. https://doi.org/10.1007/s12520-022-01712-1.

Palmqvist, P., Torregrosa, V., Pérez-Claros, J.A., Martínez-Navarro, B., Turner, A., 2007. A re-evaluation of the diversity of *Megantereon* (Mammalia, Carnivora, Machairodontinae) and the problem of species identification in extinct carnivores. J. Vertebr. Paleontol. 27 (1), 160–175. https://doi.org/10.1671/0272-4634(2007)27[160:AROTDO]2.0.CO;2.

Pante, M.C., de la Torre, I., 2018. A hidden treasure of the lower Pleistocene at Olduvai Gorge, Tanzania: the leakey HWK EE assemblage. J. Hum. Evol. 120, 114–139. https://doi.org/10.1016/j.jhevol.2017.06.006.

Pineda, A., Saladié, P., Huguet, R., Cáceres, I., Rosas, A., Estalrrich, A., García-Tabernero, A., Vallverdú, J., 2017. Changing competition dynamics among predators at the late Early Pleistocene site Barranc de la Boella (Tarragona, Spain). Palaeogeogr. Palaeoclimatol. Palaeoecol. 477, 10–26. https://doi.org/10.1016/j.palaeo.2017.03.030.

Platt, N.H., 1989. Lacustrine carbonates and pedogenesis: sedimentology and origin of palustrine deposits from the early cretaceous Rupelo formation, W Cameros basin, N Spain. Sedimentology 36 (4), 665–684. https://doi.org/10.1111/j.1365-3091.1989.tb02092.x.

Potts, R., Behrensmeyer, A., Ditchfield, P., 1999. Paleolandscape variation and early Pleistocene hominid activities: Members 1 and 7, Olorgesailie formation, Kenya. J. Hum. Evol. 37, 747–788. https://doi.org/10.1006/jhev.1999.0344.

Rodríguez-Martín, M., Lagüela, S., González-Aguilera, D., Rodríguez-Gonzálvez, P., 2015. Procedure for quality inspection of welds based on macro-photogrammetric three-dimensional reconstruction. Opt. Laser Technol. 73, 54–62.

Rohlf, F.J., Slice, D.E., 1990. Extension of the Procrustes method for the optimal superimposition of landmarks. Syst. Biol. 39, 40–59.

Ros-Montoya, S., 2010. Los proboscídeos del Plio-Pleistoceno de las cuencas de Guadix-Baza y Granada. Universidad de Granada, Granada (Ph.D. Dissertation).

Saarinen, J., Karme, A., Cerling, T., Uno, K., Säilä, L., Kasiki, L., Ngene, S., Obari, T., Manthi, F.K., Mbua, E., Fortelius, M., 2015. A new tooth wear-based dietary analysis method for Proboscidea (Mammalia). J. Vertebr. Paleontol. 35 (3), e918546 https://doi.org/10.1080/02724634.2014.918546.

Saarinen, J., Oksanen, O., Zliobaité, I., Fortelius, M., DeMiguel, D., Azanza, B., Bocherens, H., Luzón, C., Solano-García, J., Yravedra, J., Courtenay, Ll, Blain, H.A., Sánchez-Bandera, C., Serrano-Ramos, A., Rodriguez-Alba, J.J., Viranta, S., Barsky, D., Tallavaara, M., Oms, O., Agustí, J., Ochando, J., Carrion, J., Jiménez-Arenas, J.M., 2021. Pliocene to Middle Pleistocene climate history in the Guadix-Baza Basin, and the environmental conditions of early Homo dispersal in Europe. Quat. Sci. Rev. 268, 107132 https://doi.org/10.1016/j.jasrep.2021.103252.

Sánchez-Bandera, C., Fagoaga, A., Serrano-Ramos, A., Solano-García, J., Barsky, D., DeMiguel, D., Ochando, J., Saarinen, J., Piñero, P., Lozano-Fernández, I., Courtenay, L.A., Luzón, C., Bocherens, H., Yravedra, J., Fortelius, M., Agustí, J., Carrión, J.S., Oms, O., Blain, H.A., Jiménez-Arenas, J.M., 2023. Glacial/interglacial climate variability in southern Spain in the late Early Pleistocene and climate backdrop for early Homo in Europe. Palaeogeogr. Palaeoclimatol. Palaeoecol. 625, 111688 https://doi.org/10.1016/j.palaeo.2023.11688.

Schiffer, M.B., 1985. Is there a "pompeii premise" in archaeology? J. Anthropol. Res. 41, 18–41.

Semaw, S., Rogers, M.J., Simpson, S.W., Levin, N., Quade, J., Dunbar, N., McIntosh, W. C., Cáceres, I., Stinchcomb, G.E., Holloway, R.L., Brown, F.H., Butler, R.F., Stout, D., Everett, M., 2020. Co-occurrence of Acheulian and Oldowan artifacts with Homo erectus cranial fossils from Gona, Afar, Ethiopia. Sci. Adv. 6 (10), eaaw4694 https://doi.org/10.1126/sciadv.aaw4694.

Spinar, Z.V., 1996. Life before Man. Trade Paperback, Revised edition.

Stansfield, F.J., 2015. A novel objective method of estimating the age of mandibles from African elephants (*Loxodonta africana africana*). PLoS One 10, e0124980. https://doi.org/10.1371/journal.pone.0124980.

Starkovich, B.M., Cuthbertson, P., Kitagawa, K., Thompson, N., Konidaris, G.E., Rots, V., 2021. Minimal tools, maximum meat: a pilot experiment to butcher an elephant foot and make elephant bone tools using lower paleolithic stone tool Technology. Ethnoarchaeology 12, 118–147. https://doi.org/10.1080/19442890.2020.1864877.

Stoops, G., 2003. Guidelines for Analysis and Description of Soil and Regolith Thin Sections. Soil Science Society of America Inc., Madison, Wisconsin, USA.

Surovell, T.A., Waguespack, N.M., Brantingham, P.J., 2005. Global archaeological evidence for proboscidean overkill. Proc. Natl. Acad. Sci. USA 102 (17), 6231–6236. https://doi.org/10.1073/pnas.050194710.

Tappen, M., Bukhsianidze, M., Ferring, R., Coil, R., Lordkipanidze, D., 2022. Life and death at Dmanisi, Georgia: taphonomic signals from the fossil mammals. J. Hum. Evol. 171, 103249 https://doi.org/10.1016/j.jhevol.2022.103249.

Toro-Moyano, I., Lumley, H., de Barrier, P., Barsky, D., Cauche, D., Celiberti, V., Grégoire, S., Lebègue, F., Mestour, B., Moncel, M.H., Cléré, D., Dainat, D., Fauquembergue, E., Fernández, E., Fregier, C., Hildisey, F., Licht, M.H., Magnaldi, B., Montesinos, M., Monzó, D., Rey, M., 2010. Las industrias líticas arcaicas de Barranco León y Fuente Nueva 3: Orce, cuenca de Guadix-Baza,

Andalucía, España. In: Toro, I., Martínez-Navarro, B., Agustí, J. (Eds.), Ocupaciones humanas en el Pleistoceno Inferior y Medio de la Cuenca de Guadix-Baza. Consejería de Cultura, Sevilla, pp. 391–582.

Toro-Moyano, I., Barsky, D., Cauche, D., Celiberti, V., Grégoire, S., Lebegue, F., Moncel, M.H., de Lumley, H., 2011. The archaic stone-tool industry from Barranco León and Fuente Nueva 3, (Orce, Spain): evidence of the earliest hominin presence in southern Europe. Quat. Int. 243, 80–91.

Toro-Moyano, I., Martínez-Navarro, B., Agustí, J., Souday, C., Bermúdez de Castro, J.M., Martínón, M., Fajardo, B., Duval, M., Falguères, C., Oms, O., Parés, J.M., Anadón, P., Julià, R., García, J.M., Moigne, A.M., Espigares, P., Ros-Montoya, S., Palmqvist, P., 2013. The oldest human fossil in Europe, from Orce (Spain). J. Hum. Evol. 65, 1–9. https://doi.org/10.1016/j.jhevol.2013.01.012.

Turner, A., Antón, M., 1997. The Big Cats and Their Fossil Relatives. Columbia University Press, New York.

Vepraskas, M.J., Lindbo, D.L., Stolt, M.H., 2018. Chapter 15 - redoximorphic features. In: Stoops, G., Marcelino, V., Mees, F. (Eds.), Interpretation of Micromorphological Features of Soils and Regoliths, second ed. Elsevier, pp. 425–445. https://doi.org/10.1016/B978-0-444-63522-8.00015-2.

Villagran, X.S., Huisman, D.J., Mentzer, S.M., Miller, C.E., Jans, M.M., 2017. Bone and other skeletal tissues. In: Nicosia, C., Stoops, G. (Eds.), Archaeological Soil and Sediment Micromorphology. John Wiley & Sons, Ltd, pp. 9–38. https://doi.org/10.1002/9781118941065.ch1.

Waters, M.R., Stafford, T.W., McDonald, H.G., Gustafson, C., Rasmussen, M., Cappellini, E., Olsen, J.V., Szklarczyk, D., Jensen, L.J., Gilbert, M.T.P., Willerslev, E., 2011. Pre-Clovis mastodon hunting 13,800 years ago at the Manis site, Washington. Science 334 (6054), 351–353. https://doi:10.1126/science.1207663.

White, P.A., Diedrich, C.G., 2012. Taphonomy story of a modern African elephant Loxodonta africana carcass on a lakeshore in Zambia (Africa). Quat. Int. 276–277, 287–296. https://doi.org/10.1016/j.quaint.2012.07.025.

Wieder, M., Yaalon, D.H., 1982. Micromorphological fabrics and developmental stages of carbonate nodular forms related to soil characteristics. Geoderma 28, 203–220. https://doi.org/10.1016/0016-7061(82)90003-9.

Wojtal, P., Haynes, G., Klimowicz, J., Sobczyk, K., Tarasiuk, J., Wroński, S., Wilczyński, J., 2019. The earliest direct evidence of mammoth hunting in Central Europe, the Kraków Spadzista site (Poland). Quat. Sci. Rev. 213, 162–166.

Yravedra, J., Domínguez-Rodrigo, M., Santonja, M., Pérez-González, A., Panera, J., Rubio-Jara, S., 2010. Cut marks on the MP elephant carcass of Aridos 2 (Madrid, Spain). J. Archaeol. Sci. 37, 2469. https://doi.org/10.1016/j.jas.2010.05.007, 247.

Yravedra, J., Panera, J., Rubio-Jara, S., Manzano, I., Expósito, A., Pérez-González, A., Soto, E., López-Recio, M., 2014. Neanderthal and Mammuthus interactions at EDAR Culebro 1 (Madrid, Spain. J. Archaeol. Sci. 42, 500–508. https://doi.org/10.1016/j.jas.2013.11.011.

Yravedra, J., Aramendi, J., Maté-González, M.Á., Courtenay, L.A., González-Aguilera, D., 2018. Differentiating percussion pits and carnivore tooth pits using 3D reconstructions and geometric morphometrics. PLoS One 13 (3), e0194324. https://doi.org/10.1371/journal.pone.0194324.

Yravedra, J., Rubio-Jara, S., Panera, J., Martos, J.A., 2019. Hominins and proboscideans in the lower and Middle palaeolithic in the central iberian Peninsula. Quat. Int. 520, 140–156. https://doi.org/10.1016/j.quaint.2017.12.002.

Yravedra, J., Rubio-Jara, S., Courtenay, Ll, Martos, J.A., 2020. Mammal butchery by Homo erectus at the Lower Pleistocene acheulean site of Juma's korongo 2 (JK2), bed III, Olduvai Gorge, Tanzania. Quat. Sci. Rev. 249, 1. https://doi.org/10.1016/j.quascirev.2020.106612.

Yravedra, J., Solano, J.A., Courtenay, L.A., Saarinen, J., Linares-Matás, G., Luzón, C., Serrano-Ramos, A., Herranz-Rodrigo, D., Cámara, J.M., Ruiz, A., Titton, S., Rodríguez-Alba, J.J., Mielgo, C., Blain, H.-A., Agusti, J., Sánchez-Bandera, C., Montilla, E., Toro-Moyano, I., Fortelius, M., Jiménez- Arenas, J.M., 2021. Use of meat resources in the early Pleistocene assemblages from Fuente Nueva 3 (Orce, Granada, Spain). Archaeol. Anthropol. Sci. 13, 213. https://doi.org/10.1007/s12520-021-01461-7.

Yravedra, J., Courtenay, L.A., Herranz-Rodrigo, D., Linares-Matás, G.J., Rodríguez-Alba, J.J., Estaca-Gómez, V., Luzón, C., Serrano-Ramos, A., Maté-González, M.A., Solano, J.A., González-Aguilera, D., Jiménez-Arenas, J.M., 2022. Taphonomic characterisation of tooth marks of extinct Eurasian carnivores through Geometric Morphometric. Sci. Bull. 67, 1644–1648. https://doi.org/10.1016/j.scib.2022.07.017.

Zaidner, Y., 2013. Adaptive flexibility of oldowan hominins: secondary use of flakes at Bizat Ruhama, Israel. PLoS One 8 (6), e66851. https://doi.org/10.1371/journal.pone.0066851.